SLAC–PUB–8364
February 2000

Properties of Gamma-Ray Burst Time Profiles Using Pulse Decomposition Analysis*

Andrew Lee and Elliott D. Bloom
Stanford Linear Accelerator Center, Stanford University, Stanford, CA 94309

Vahé Petrosian
Center for Space Science and Astrophysics, Varian 302c, Stanford University, Stanford, CA 94305-4060

Abstract

The time profiles of many gamma-ray bursts consist of distinct pulses, which offers the possibility of characterizing the temporal structure of these bursts using a relatively small set of pulse shape parameters. This pulse decomposition analysis has previously been performed on a small sample of bright long bursts using binned data from BATSE, which comes in several data types, and on a sample of short bursts using the BATSE Time-Tagged Event (TTE) data type. We have developed an interactive pulse-fitting program using the phenomenological pulse model of Norris, *et al.* and a maximum-likelihood fitting routine. We have used this program to analyze the Time-to-Spill (TTS) data for all bursts observed by BATSE up through trigger number 2000, in all energy channels for which TTS data is available. We present statistical information on the attributes of pulses comprising these bursts, including relations between pulse characteristics in different energy channels and the evolution of pulse characteristics through the course of a burst. We carry out simulations to determine the biases that our procedures may introduce. We find that pulses tend to have shorter rise times than decay times, and tend to be narrower and peak earlier at higher energies. We also find that pulse brightness, pulse width, and pulse hardness ratios do not evolve monotonically within bursts, but that the ratios of pulse rise times to decay times tends to decrease with time within bursts.

Submitted to Astrophysical Journal

*Work supported by Department of Energy contract DE–AC03–76SF00515.

Properties of Gamma-Ray Burst Time Profiles Using Pulse Decomposition Analysis

Andrew Lee and Elliott D. Bloom

Stanford Linear Accelerator Center, Stanford University, Stanford, California 94309

Vahé Petrosian

Center for Space Science and Astrophysics, Varian 302c, Stanford University, Stanford, CA 94305-4060 [1]

ABSTRACT

The time profiles of many gamma-ray bursts consist of distinct pulses, which offers the possibility of characterizing the temporal structure of these bursts using a relatively small set of pulse shape parameters. This pulse decomposition analysis has previously been performed on a small sample of bright long bursts using binned data from BATSE, which comes in several data types, and on a sample of short bursts using the BATSE Time-Tagged Event (TTE) data type. We have developed an interactive pulse-fitting program using the phenomenological pulse model of Norris, *et al.* and a maximum-likelihood fitting routine. We have used this program to analyze the Time-to-Spill (TTS) data for all bursts observed by BATSE up through trigger number 2000, in all energy channels for which TTS data is available. We present statistical information on the attributes of pulses comprising these bursts, including relations between pulse characteristics in different energy channels and the evolution of pulse characteristics through the course of a burst. We carry out simulations to determine the biases that our procedures may introduce. We find that pulses tend to have shorter rise times than decay times, and tend to be narrower and peak earlier at higher energies. We also find that pulse brightness, pulse width, and pulse hardness ratios do not evolve monotonically within bursts, but that the ratios of pulse rise times to decay times tends to decrease with time within bursts.

Subject headings: gamma rays: bursts—methods: data analysis

1. Introduction

There has been considerable recent progress in the study of gamma-ray bursts. Much of this results from the detection of bursts by BeppoSAX with good locations that have allowed

[1] Also Astronomy Program and Department of Physics.

the detection of counterparts at other wavelengths. This has allowed measurements of redshifts that have firmly established that these bursts are at cosmological distances. However, only a few redshifts are known, so there is still much work to be done in determining the mechanisms that produce gamma-ray bursts. Investigation of time profiles and spectra can shed new light on this subject.

The vast majority of gamma-ray bursts that have been observed have been observed *only* by BATSE. This data can be classified into three major types: burst locations with relatively large uncertainties, temporal characteristics, and spectral characteristics. Here, we shall examine temporal characteristics of bursts, along with some spectral characteristics.

The temporal structure of gamma-ray bursts exhibit very diverse morphologies, from single simple spikes to extremely complex structures. So far, the only clear division of bursts based on temporal characteristics that has been found is the bimodal distribution of the T_{90} and T_{50} intervals, which are measures of burst durations (Kouveliotou et al. 1993; Meegan et al. 1996a). In order to characterize burst time profiles, it is useful to be able to describe them using a small number of parameters.

Many burst time profiles appear to be composed of a series of discrete, often overlapping, pulses, often with a *fast rise, exponential decay* (FRED) shape (Norris et al. 1996). These pulses have durations ranging from a few milliseconds to several seconds. The different pulses might, for example, come from different spatial volumes in or near the burst source. Therefore, it may be useful to decompose burst time profiles in terms of individual pulses, each of which rises from background to a maximum and then decays back to background levels. Here, we have analyzed gamma-ray burst time profiles by representing them in terms of a finite number of pulses, each of which is described by a small number of parameters. The BATSE data used for this purpose is described in Section 2. The basic characteristics of the time profiles based on the above model are described in Section 3 and some of the correlations between these characteristics are described in Section 4. (Further analysis of these and other correlations and their significance are discussed in an accompanying paper, Lee et al. (2000).) Finally, a brief discussion is presented in Section 5.

2. The BATSE Time-to-Spill Data

The BATSE Time-to-Spill (TTS) burst data type records the times required to accumulate a fixed number of counts, usually 64, in each of four energy channels (Meegan 1991). These time intervals give fixed multiples of the reciprocals of the average count rates during the spill intervals. There has been almost no analysis done using the TTS data because it is less convenient to use with standard algorithms than the BATSE Time-Tagged Event (TTE) data or the various forms of binned BATSE data. The TTS data use the limited memory on board the CGRO more efficiently than do the binned data types because at lower count rates, it stores spills less frequently, with each spill having the same constant fractional statistical error. On the other hand, the binned

data types always store binned counts at the same intervals, so that at low count rates the binned counts have a large fractional statistical error. The variable time resolution of the TTS data ranges from under 50 ms at low background rates to under 0.1 ms in the peaks of the brightest bursts. In contrast, the finest time resolution available for binned data is 16 ms for the medium energy resolution (MER) data, and then only for the first 33 seconds after the burst trigger. The TTS data can store up to 16,384 spill events (over 10^6 counts) for each energy channel, and this is almost always sufficient to record the complete time profiles of bright, long bursts. This is unlike the TTE data, which are limited to 32,768 counts in all four energy channels combined. For short bursts, the TTE data have finer time resolution than the TTS data, because it records the arrival times of individual counts with 2 μs resolution. Furthermore, the TTE data also contain data from before the burst trigger time. One reason why this is useful is that some of the shortest bursts are nearly over by the time burst trigger conditions have been met, so the TTS and MER data aren't very useful for these bursts.

Figure 1 shows a portion of the time profile of BATSE trigger number 1577 (GRB 4B 920502B) that contains a spike with duration shorter than 1 ms. The data with the finest time resolution, the time-tagged event (TTE) data, end long before the spike occurs, so the TTS data give the best representation of the spike. The binned data with the finest time resolution, the MER data with 16 ms bins, are unavailable for this burst, as are the PREB and DISCSC data with 64 ms bins.

For a Poisson process, the individual event times in the TTE data and the binned counts in the various binned data types follow the familiar exponential and the Poisson distributions, respectively. The spill times recorded in the TTS data follow the *gamma distribution*, which is the distribution of times needed to accumulate a fixed number of independent (Poisson) events occurring at a given rate. The probability of observing a spill time t_s is

$$P(t_s) \;=\; \frac{t_s^{N-1} R^N e^{-Rt_s}}{\Gamma(N)} \;, \tag{1}$$

where N is the number of events per spill and R is the rate of individual events. This probability distribution is closely related to the Poisson distribution, which gives the number of events occurring within fixed time intervals for the same process of independent individual events, such as photon arrivals.

2.1. The Pulse Model and the Pulse Fitting Procedure

We now describe the pulse model used to fit GRB time profiles, and the pulse-fitting procedure. The pulse model we use is the phenomological pulse model of Norris et al. (1996) In this model, each pulse is described by five parameters with the functional form

$$I(t) \;=\; A \exp\left(- \left| \frac{t - t_{\max}}{\sigma_{r,d}} \right|^{\nu} \right) \;, \tag{2}$$

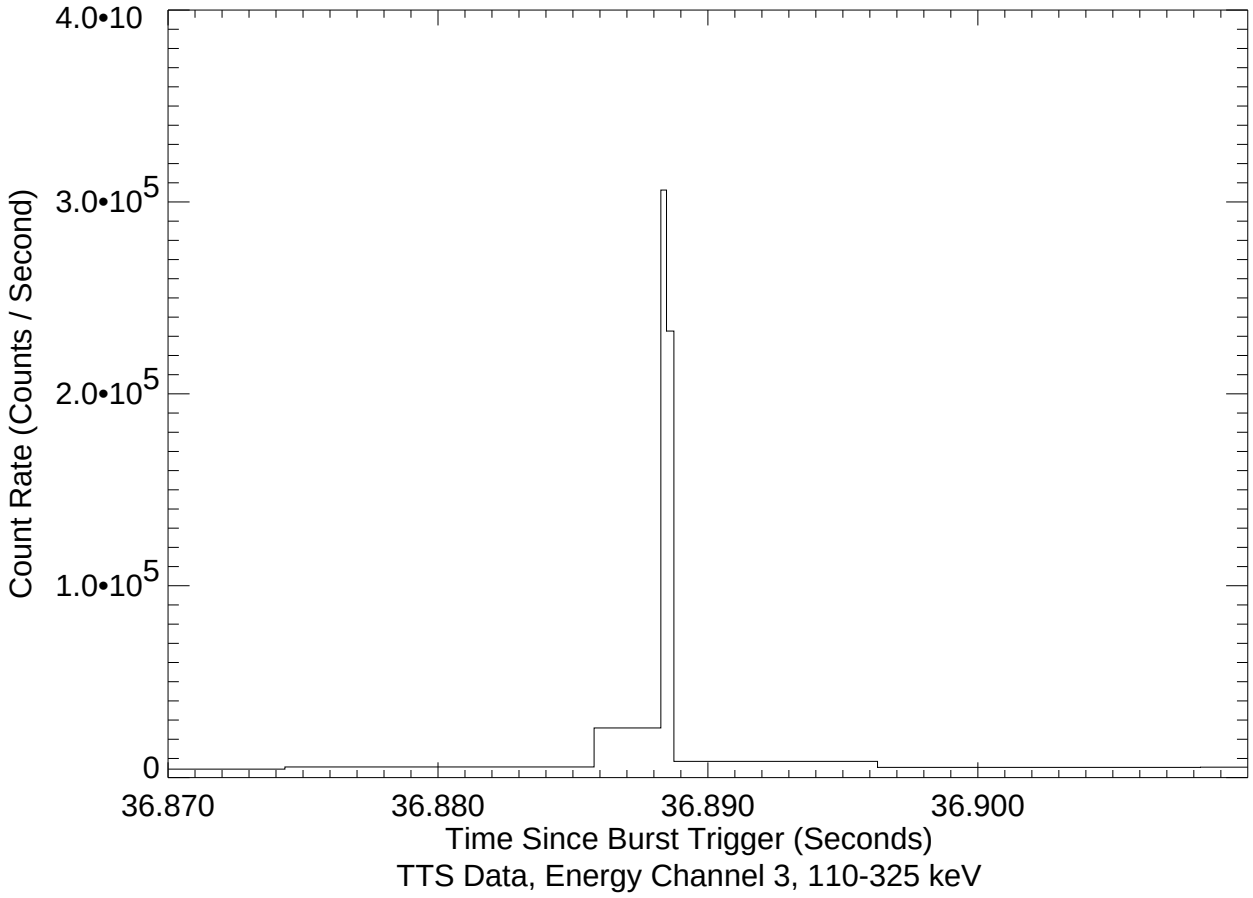

Fig. 1.— A portion of the TTS data for BATSE Trigger Number 1577 (4B 920502B). Note the fine time resolution of the TTS data for the spike more than 36 seconds after the burst trigger.

where $t_{\max}$ is the time at which the pulse attains its maximum, σ_r and σ_d are the rise and decay times, respectively, A is the pulse amplitude, and ν (the "peakedness") gives the sharpness or smoothness of the pulse at its peak. Pulses can, and frequently do, overlap. Stern et al. (1997) have used the same functional form to fit averaged time profiles (ATPs) of entire bursts.

We have developed an interactive pulse-fitting program that can automatically find initial background level and pulse parameters using a Haar wavelet denoised time profile (Donoho 1992), and allows the user to add or delete pulses graphically. The program then finds the parameters of the pulses and a background with a constant slope by using a maximum-likelihood fit for the gamma distribution (equation 1) that the TTS spill times follow (Lee et al. 1996, 1998; Lee 2000).

The data that we use in this paper are the TTS data for all gamma-ray bursts in the BATSE 3B catalog (Meegan et al. 1996b) up to trigger number 2000, covering the period from 1991 April 21 through 1992 October 22, in all channels that are available and show time variation beyond the normal Poisson noise of the background. We fit each channel of each burst separately and obtained 574 fits for 211 bursts, with a total of 2465 pulses. In many cases, the data for a burst showed no activity in a particular energy channel, only the normal background counts, so there were no pulses to fit. This occurred most frequently in energy channel 4. In other cases, the data for a burst contained telemetry gaps or were completely missing in one or more channels, making it impossible to fit those channels.

This procedure is likely to introduce selection biases, which can be quantified through simulation. To determine these biases, we simulated a set of bursts with varying numbers of pulses with distributions of pulse and background parameters based on the observed distributions in actual bursts. We generated independent counts according to the simulated time profiles to create simulated TTS data, which we subjected to the same pulse-fitting procedure used for the actual BATSE data. The detailed results of this simulation are discussed in the Appendix. We will contrast the results from the actual data with those from the simulations where necessary and relevant.

2.2. Count Rates and Time Resolution

The time resolution of the TTS data can be determined from the fitted background rates and the amplitudes of the individual pulses (discussed later in Subsection 3.3), at both the background levels and at the peaks of the pulses. Table 1, columns (a) show the percentage of bursts in our fitted sample where the time resolution at background levels and at the peak of the highest amplitude pulse are finer than 64 ms and 16 ms, the time resolutions of the more commonly used DISCSC and MER data, respectively. The background rates are taken at the time of the burst trigger, and ignore the fitted constant slope of the background. The rates at the peaks of the highest amplitude pulses include the background rates at the peak times of the pulses calculated with the background slopes. However, these rates ignore overlapping pulses, so the actual time resolution will be finer since the actual count rates will be higher. Note that even at background levels, the TTS data

always have finer time resolution than the DISCSC data, except in energy channel 4 where the DISCSC data have finer time resolution for 32% of the bursts in our sample.

Table 1, columns (b) show the percentage of individual pulses where the TTS data have time resolution finer than 16 ms and 64 ms at the pulse peaks. Again, the count rates include the fitted background rates at the peak times of the pulses but ignore overlapping pulses. For all individual pulses, the TTS data have finer time resolution at their peaks than the DISCSC data.

3. General Characteristics of Pulses in Bursts

In this section we describe characteristics of pulses in individual bursts and in the sample as a whole.

3.1. Numbers of Pulses

The number of pulses in a fit range from 1 to 43, with a median of 2 pulses per fit in energy channels 1, 2, and 4, and a median of 3 pulses per fit in energy channel 3. (See Figure 2.) The numbers of pulses per fit follows the trend of pulse amplitudes, which we shall see tend to be highest in energy channel 3, followed in order by channels 2, 1, and 4, respectively. This appears to occur because higher amplitude pulses are easier to identify above the background, and is consistent with the simulation results shown in the Appendix.

Norris et al. (1996) have used the pulse model of equation 2 to fit the time profiles of 45 bright, long bursts. They analyzed the BATSE PREB and DISCSC data types, which contain four-channel discriminator data with 64 ms resolution beginning 2 seconds before the burst trigger. For their selected sample of bursts, they fitted an average of 10 pulses per burst, with no time profiles consisting of only a single pulse. This number is considerably higher than the mean number of pulses per fit for our sample of bursts, probably because their sample was selected for high peak flux and long duration, which makes it easier to resolve more pulses.

3.2. Matching Pulses Between Energy Channels

To see how attributes of pulses within a burst vary with energy, it is necessary to match pulses in different energy channels. Although burst time profiles generally have similar features in different energy channels, this matching is not straightforward, since the number of pulses fitted to a burst time profile is very often different between energy channels. We have used a simple automatic algorithm for matching pulses between adjacent energy channels. This algorithm begins by taking all pulses from the channel with fewer pulses. It then takes the same number of pulses of highest amplitude from the other channel, and matches them in time order with the pulses from the channel

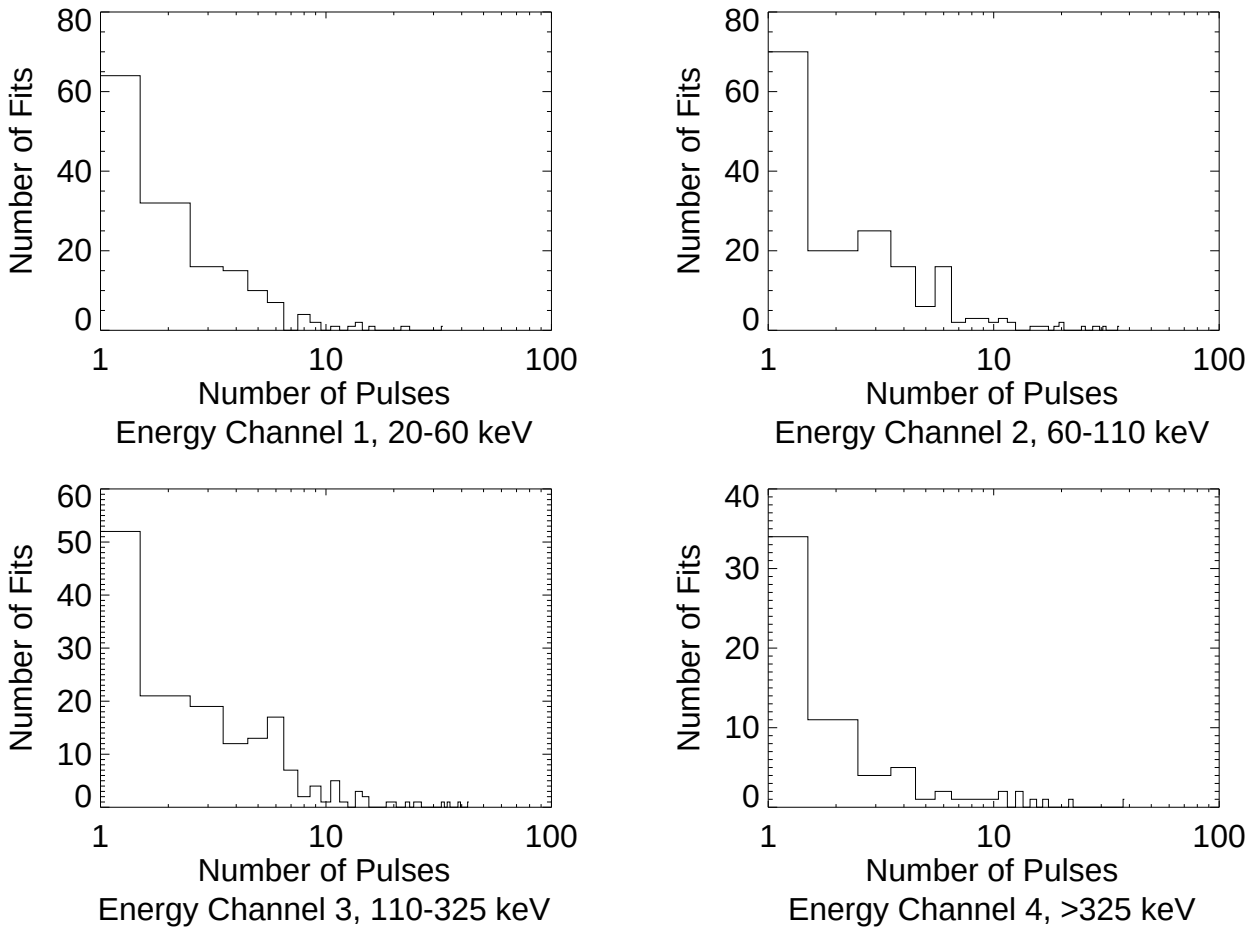

Fig. 2.— Distribution of number of pulses per burst, by energy channel. Compare with Figure 11 from simulations.

with fewer pulses. For example, the time profiles of BATSE trigger number 1577 were fitted with nine pulses in energy channel 3, and only four pulses in channel 4. This algorithm simply matches all four pulses in channel 4 in time order with the four highest amplitude pulses in channel 3. While this method will not always correctly match individual pulses between energy channels and will result in broad statistical distributions, it should still preserve central tendencies and yield useful statistical information.

3.3. Brightness Measures of Pulses: Amplitudes and Count Fluences

The amplitude of a pulse, parameter A in equation 2, is the maximum count rate within the pulse, and measures the observed intensity of the pulse, which depends on the absolute intensity of the pulse at the burst source and the distance to the burst source. The amplitudes of the fitted pulses ranged from 40 counts/second to over 500,000 counts/second. (See Table 2 and Figure 3.) Pulses tend to have the highest amplitudes in energy channel 3, followed in order by channels 2, 1, and 4, in agreement with Norris et al. (1996). The central 68% of the pulse amplitude distributions span a range of about one order of magnitude in each of the four energy channels, with a somewhat greater range in channel 3. We will see in the Appendix that the fitting procedure tends to miss pulses with low amplitudes, so that the distributions shown may be strongly affected by selection effects in the fitting procedure.

The amplitude of the highest amplitude pulse in a burst is an approximation to the instantaneous peak flux above background of that burst in that energy channel. The peak flux is often used as an indicator of the distance to the burst source. Since pulses can overlap, the highest pulse amplitude can be less than the actual background-subtracted peak flux. The BATSE burst catalogs give background-subtracted peak fluxes for 64, 256, and 1024 ms time bins in units of photons/cm^2/second, for which effects such as the energy acceptances of the detectors and the orientation of the spacecraft and hence the detectors relative to the source have been accounted for and removed. The BATSE burst catalog also lists raw peak count rates that are not background-subtracted or corrected for any of the effects described, averaged over 64, 256, and 1024 ms time bins in the second most brightly illuminated detector for each burst. These peak count rates are primarily useful for comparison with the BATSE event trigger criteria. In some bursts, the highest pulses are considerably narrower than the shortest time bins used to measure peak flux in the BATSE burst catalog. For these bursts, these peak fluxes will be lower than the true peak flux, and the fitted pulse amplitudes are likely to be a better measure of the true peak flux. The distributions of the highest pulse amplitudes are shown in Table 3 and Figure 4. Since BATSE selectively triggers on events with high peak flux, the distributions must be strongly affected by the trigger criteria.

Figure 5 shows the number of pulses in each fit plotted against the amplitudes of all of the pulses comprising each fit. It shows that in fits with more pulses, the minimum pulse amplitude, which can be seen from the left boundary of the distribution, tends to be higher. This could result in part from intrinsic properties of the burst sources, but may also result at least in part from

Table 1. Percentage of (a) Bursts and (b) Individual Pulses with Time Resolution < 64 ms, < 16 ms.

	(a) Bursts				(b) Individual	
Energy	Background		Highest Amplitude Pulse		Pulses	
Channel	% < 64 ms	% < 16 ms	% < 64 ms	% < 16 ms	% < 64 ms	% < 16 ms
1	100%	16%	100%	80%	100%	80%
2	100%	8%	100%	75%	100%	68%
3	100%	3%	100%	67%	100%	62%
4	68%	1%	100%	30%	100%	42%
All	96%	8%	100%	69%	100%	65%

Table 2. Characteristics of Distribution of Pulse Amplitudes for All Pulses in All Bursts Combined.

Energy Channel	Min. Amp. (Counts / Sec.)	Median Amp. (Counts / Sec.)	Max. Amp. (Counts / Sec.)	Ratio 84%ile / 16%ile
1	47	2200	136,000	10.8
2	85	2700	543,000	12.9
3	93	3000	250,000	16.2
4	43	1900	63,000	11.8

Table 3. Characteristics of Distribution of Pulse Amplitudes for Highest Amplitude Pulse in Each Burst.

Energy Channel	Min. Amp. (Counts / Sec.)	Median Amp. (Counts / Sec.)	Max. Amp. (Counts / Sec.)	Ratio 84%ile / 16%ile
1	241	2200	136,000	11.1
2	148	2800	543,000	9.9
3	116	3500	250,000	12.4
4	82	1500	63,000	18.8

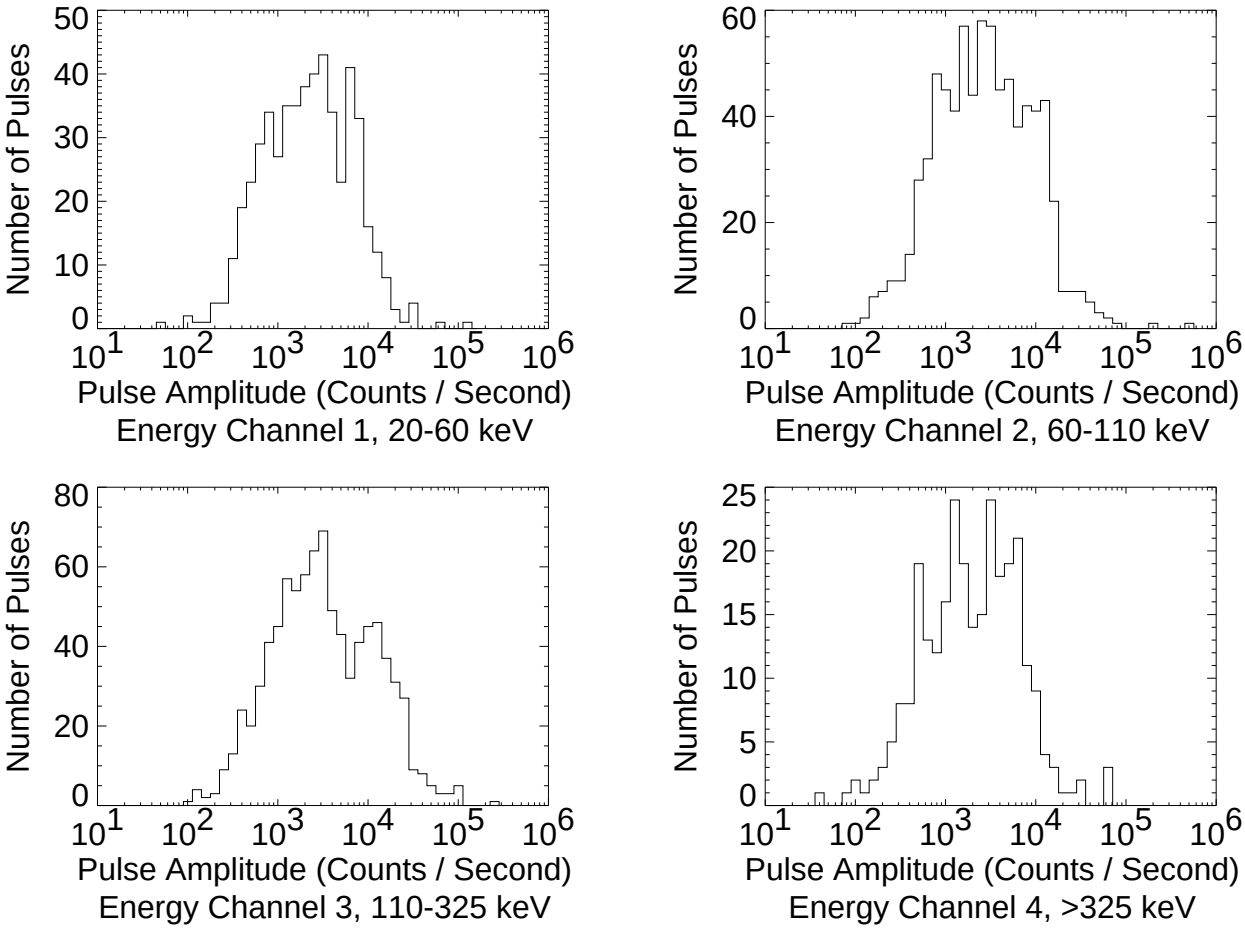

Fig. 3.— Distribution of pulse amplitudes for all pulses from all bursts, by energy channel. Note that the rapid decline at low amplitudes is partly due to the BATSE triggering procedure and partly due to the fitting procedure. See Figure 14.

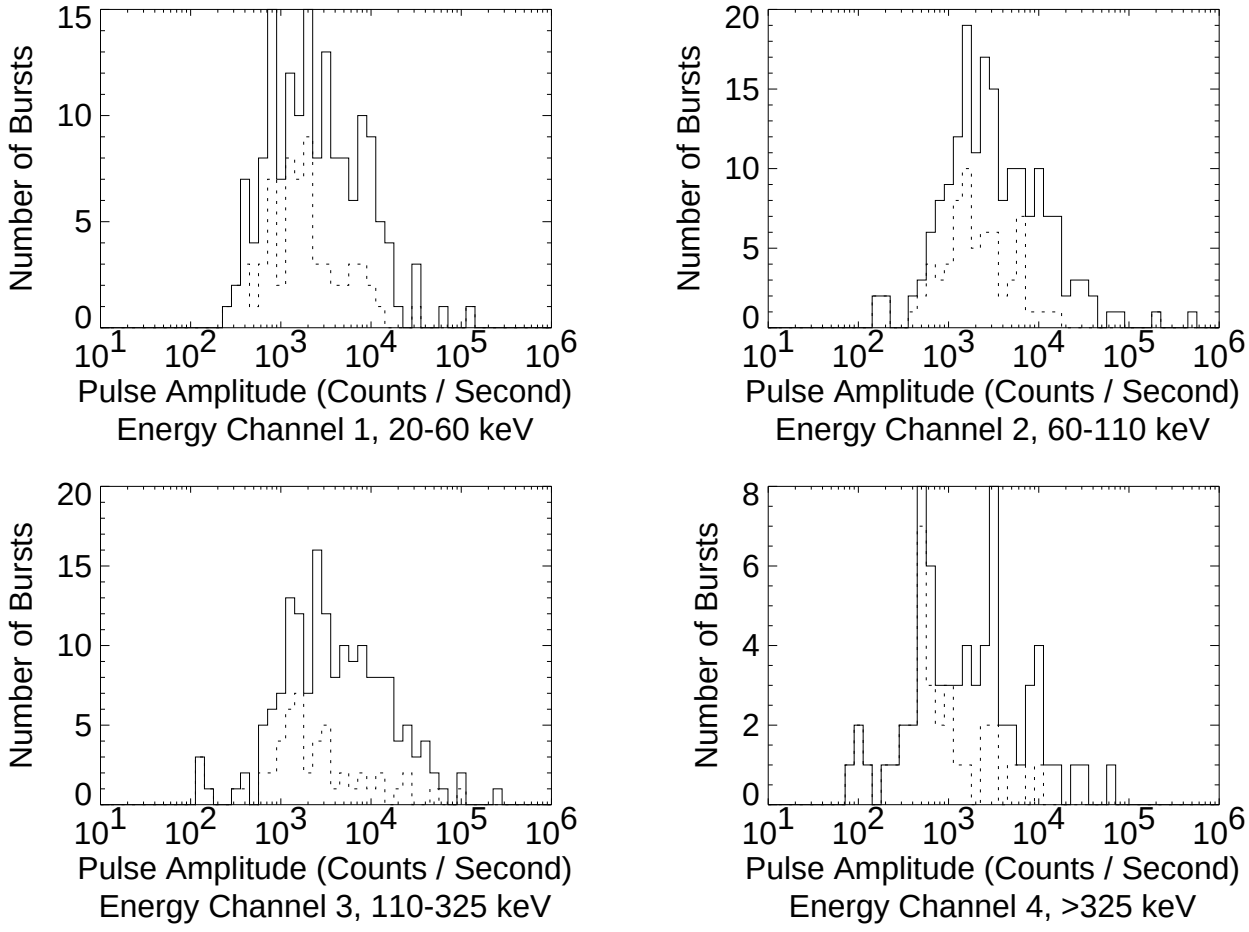

Fig. 4.— Distribution of pulse amplitudes, highest amplitude pulse in each burst, by energy channel. Dashed lines are bursts containing only a single pulse. The more rapid decline at low amplitudes as compared with that in Figure 3 is due to the stronger influence of the BATSE triggering procedure. The fitting procedure has a weaker influence here.

a selection effect: In a complex time profile with many overlapping pulses, low amplitude pulses, which have poor signal-to-noise ratios, will be more difficult to resolve, while in a less complex time profile, they will be easier to resolve. This hypothesis appears to be confirmed by the simulation results shown in the Appendix. Table 4, columns (a) give the Spearman rank-order correlation coefficients, commonly denoted as r_s, for the joint distribution of pulse amplitudes and numbers of pulses in the corresponding bursts shown in Figure 5, as well as the probability that a random data set of the same size with no correlation between the two variables would produce the observed value of r_s. It shows strong positive correlations between pulse amplitudes and the number of pulses in the fit for all energy channels. These correlations appear to be stronger than those arising in the fits to simulations shown in Table 16, columns (a).

The area under the light curve of a pulse gives the total number of counts contained in the pulse, which is its count fluence. It is given in terms of the pulse parameters and the gamma function by

$$\mathcal{F} = A \int_{-\infty}^{\infty} I(t)dt = A \frac{\sigma_r + \sigma_d}{\nu} \Gamma\left(\frac{1}{\nu}\right). \tag{3}$$

The count fluence is a measure of the observed integrated luminosity of the pulse, which depends on the total number of photons emitted by the source within the pulse and the distance to the burst source. We will see in the Appendix that the fitting procedure tends to miss pulses with low count fluences.

Figure 6 shows the number of pulses in each fit versus the count fluences of the individual pulses. It shows that in bursts containing more pulses, the individual pulses tend to contain fewer counts. We shall see in the next section that pulses tend to be narrower in more complex bursts. This result for count fluences implies that the tendency for pulses to be narrower is stronger than the tendency for pulses to have higher amplitudes in more complex bursts. Table 4, columns (b) show that the corresponding negative correlations between pulse count fluences and numbers of pulses per fit are statistically significant in energy channels 1 and 2, but not in channels 3 and 4.

Table 4. Correlation Between Number of Pulses per Burst and (a) Amplitudes, (b) Count Fluences, and (c) Widths of All Pulses.

Energy	(a) Amplitude		(b) Count Fluence		(c) Width	
Channel	r_s	Prob.	r_s	Prob.	r_s	Prob.
1	0.37	3.9×10^{-18}	-0.17	9.2×10^{-5}	-0.36	1.8×10^{-17}
2	0.36	1.8×10^{-24}	-0.20	3.4×10^{-8}	-0.35	8.0×10^{-24}
3	0.30	4.2×10^{-20}	-0.04	0.21	-0.23	9.4×10^{-12}
4	0.45	2.2×10^{-15}	-0.13	0.027	-0.28	1.3×10^{-6}

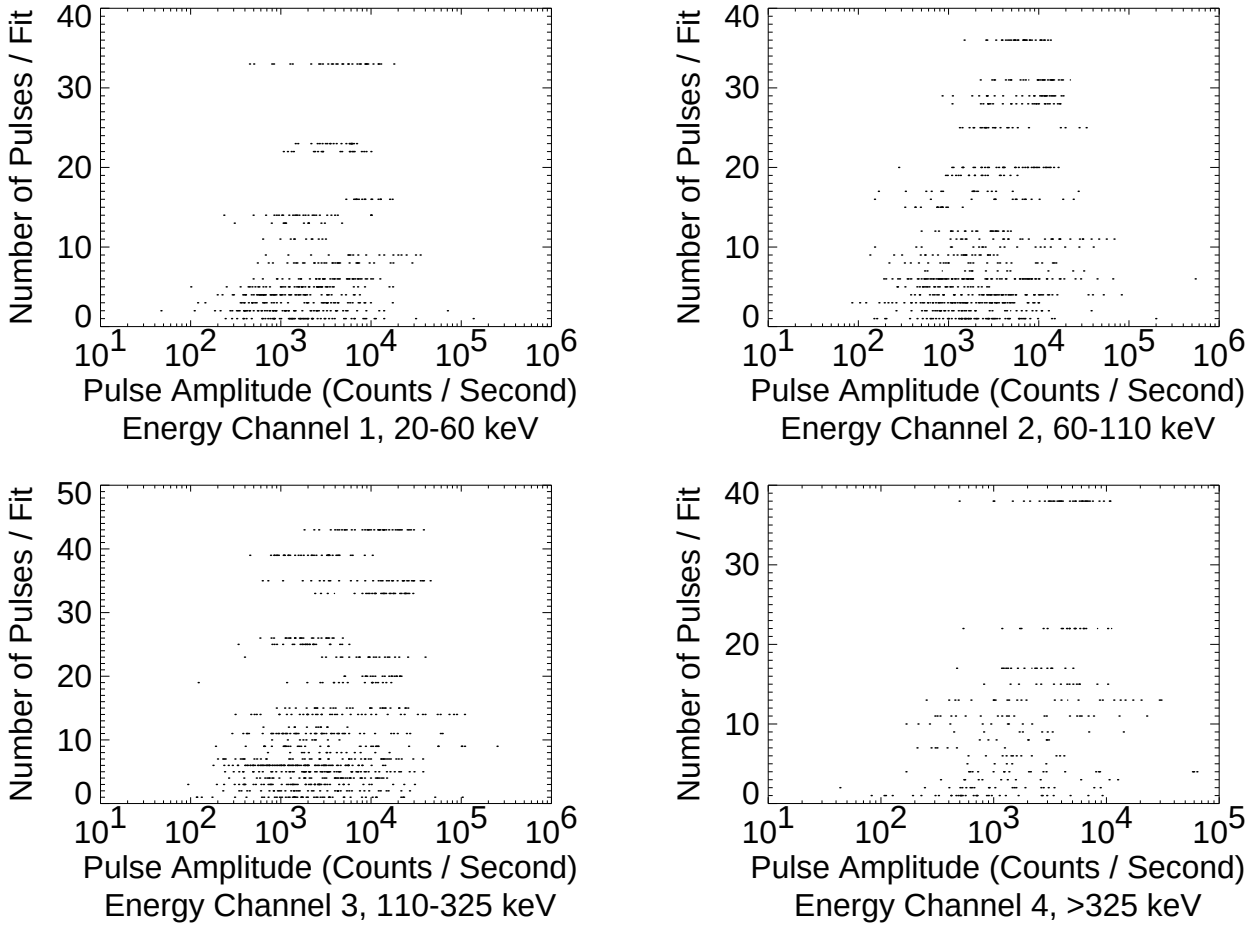

Fig. 5.— Number of pulses per burst versus pulse amplitudes of all pulses, by energy channel. Compare with Figure 15 for simulated data. Note that there exists a positive correlation between the two quantities.

The fits to simulations (Figure 17 and Table 16, columns (b)) do not show the same tendency, so this most likely is not caused by selection effects in the pulse-fitting procedure.

3.4. Pulse Widths and Time Delays

Timescales in gamma-ray bursts are likely to be characteristic of the physical processes that produce them. However, since some, and possibly all, bursts are produced at cosmological distances, all observed timescales will be affected by cosmological time dilation, and won't represent the physical timescales at the sources.

3.4.1. Pulse Widths

The most obvious timescale that appears in the pulse decomposition of gamma-ray burst time profiles is the pulse width, or duration. We shall measure the duration, or width, of a pulse using its full width at half maximum (FWHM), which is given by

$$T_{\rm FWHM} = (\sigma_r + \sigma_d)(\ln 2)^{\frac{1}{\nu}}. \tag{4}$$

The distributions of the pulse widths, which are shown in Figure 7 and columns (a) of Table 5, peak near one second in all energy channels, with no sign of the bimodality seen in total burst durations mentioned above. Pulses tend to be narrower (shorter) at higher energies.

The narrowing of pulses in higher energy channels can also be measured from the ratios of pulse widths of matched pulses in adjacent energy channels, as shown in Table 6. We can test the hypothesis that pulses tend to be narrower at higher energies by computing the probability that the observed numbers of pulses width ratios less than 1 will occur by chance if pulse width ratios less than 1 and greater than 1 are equally probable. This probability can be computed from the binomial distribution, and is shown in the last column of Table 6. The table shows less narrowing than a simple comparison of median pulse widths from Table 5 would suggest, though it also shows that the hypothesis that pulses *do not* become narrower at higher energies is strongly excluded between channels 1 and 2 and between channels 2 and 3. Qualitatively similar kinds of trends have been shown to be present in individual pulses (Norris et al. 1996) and composite pulse shapes of many bursts (Link et al. 1993; Fenimore & Bloom 1995). There are, however, some quantitative differences. For example, we find that there seems to be less narrowing at higher energies; the pulse width ratios tend to be closer to 1 between energy channels 3 and 4 than for the lower energy channels (although the statistics are poorer, as with anything involving channel 4), which is the opposite of the tendency found by Norris et al. (1996). We can use the Kolmogorov-Smirnov test to determine if the distributions of pulse width ratios are the same between adjacent energy channels. These results are shown in the last column of Table 6. This test shows significant differences in the distribution of pulse widths of matched pulses between adjacent energy channels.

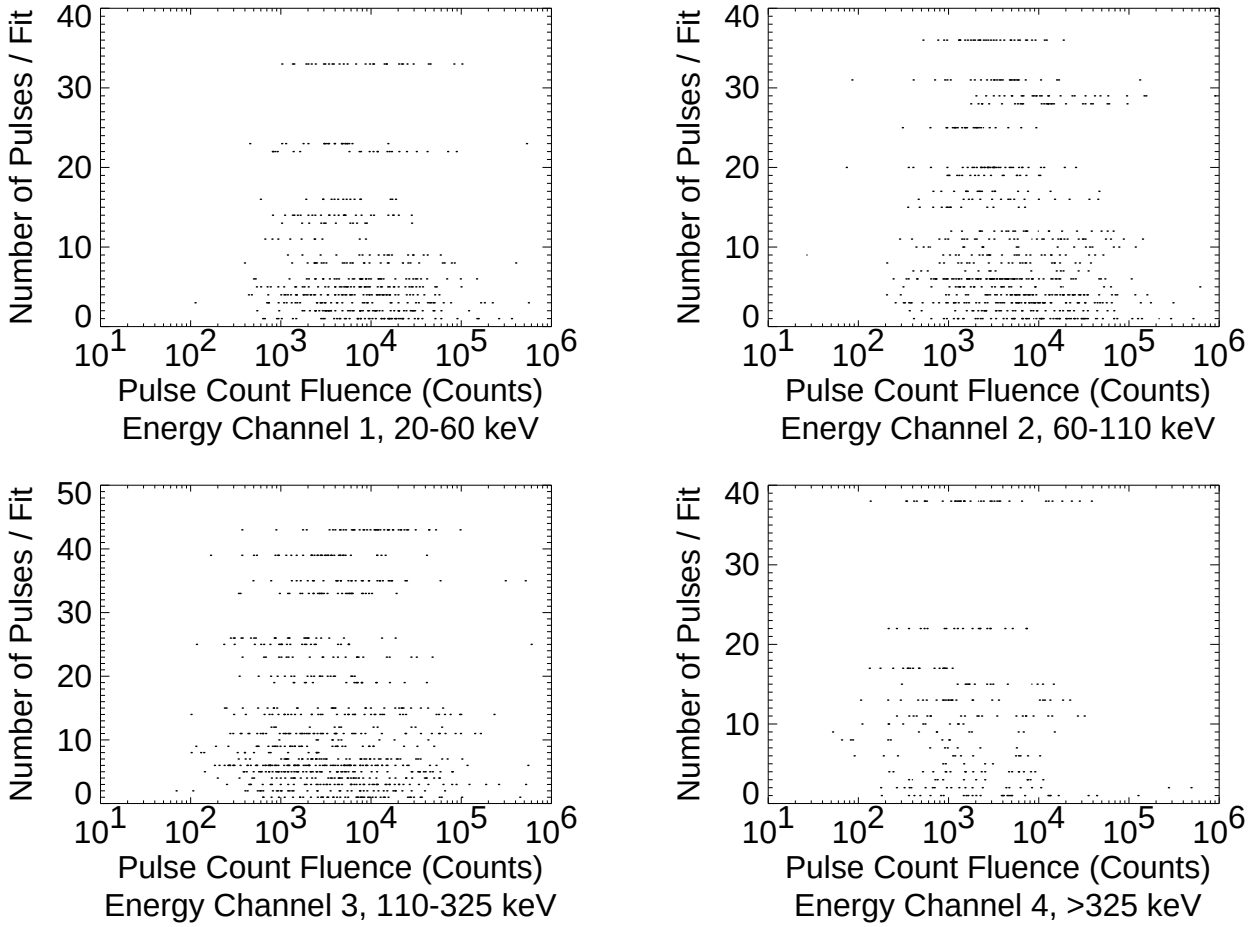

Fig. 6.— Number of pulses per burst versus count fluences of all pulses from all bursts, by energy channel. Compare with Figure 17 for simulated data. Note that there exists a negative correlation between the two quantities.

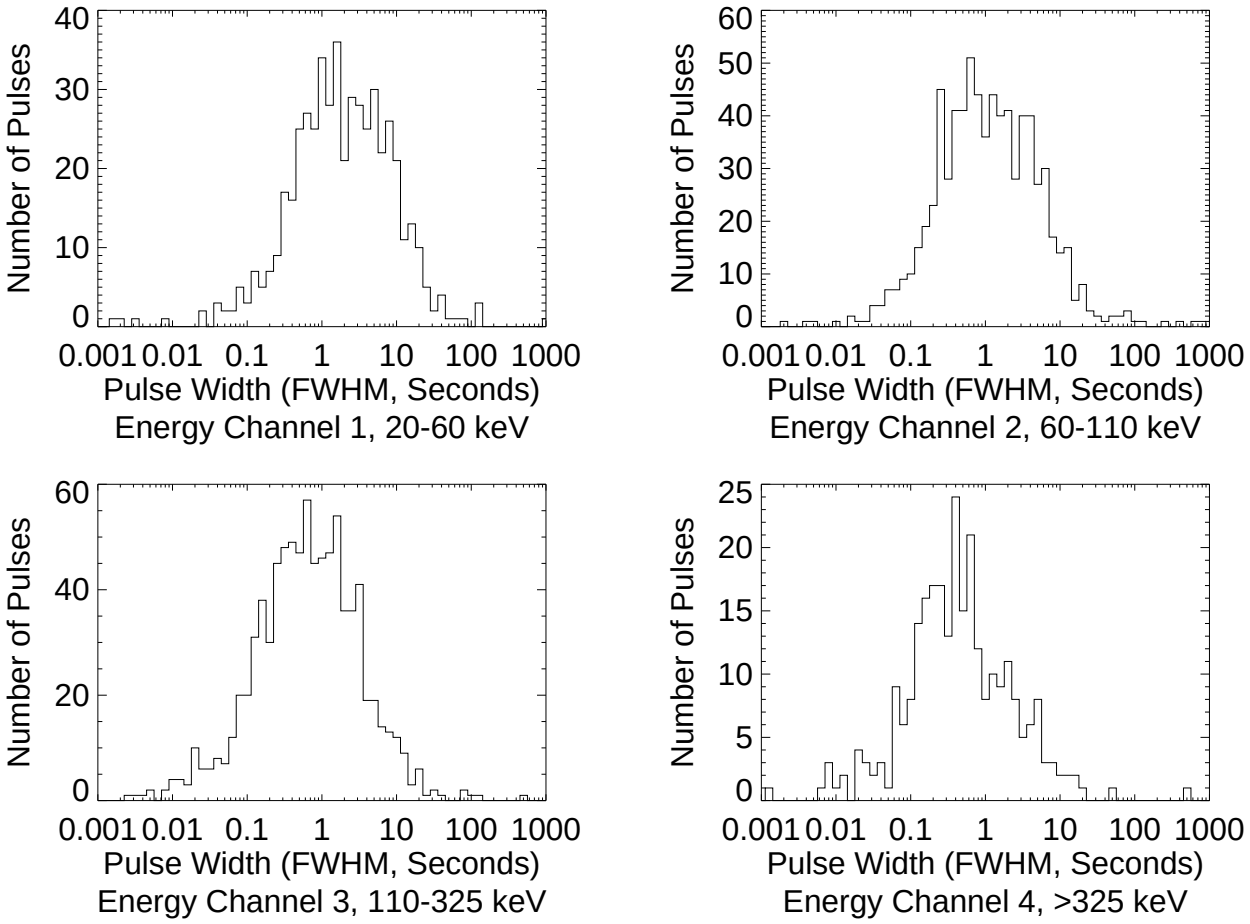

Fig. 7.— Distribution of pulse widths (FWHM) for all pulses from all bursts, by energy channel. Note that there is no indication that pulse widths have the bimodality observed in the distributions of the T_{50} and T_{90} measures of burst durations in the BATSE catalogs. Compare with the distribution for simulated bursts in Figure 18.

Table 5. Characteristics of Distribution of (a) Pulse Widths and of (b) Peakedness ν for All Pulses in All Bursts Combined.

	(a) FWHM		(b) Peakedness ν	
Energy Channel	Median (Seconds)	Ratio 84%ile / 16%ile	Median ν	Ratio 84%ile / 16%ile
1	1.86	19.9	1.22	5.3
2	1.05	23.0	1.26	5.6
3	0.68	22.9	1.26	5.7
4	0.41	21.4	1.17	5.8
All	0.90	27.0	1.25	5.6

Table 6. Ratios of Pulse Widths of Pulses Matched Between Adjacent Energy Channels.

Energy Channels	Median Width Ratio	$\% < 1$	Binom. Prob.	K-S Prob.
2 / 1	0.73	$304/446 = 68\%$	1.7×10^{-14}	1.1×10^{-5}
3 / 2	0.68	$436/625 = 70\%$	$< 10^{-16}$	8.7×10^{-7}
4 / 3	0.83	$153/258 = 59\%$	0.0028	0.62

The fact that pulse widths decrease monotonically with energy, and the signal-to-noise ratios of the different energy channels increase in order of the energy channels 3, 2, 1, 4, imply that the narrowing is caused by the burst production mechanism itself.

3.4.2. Pulse Widths and Numbers of Pulses

Figure 8 and Table 4, columns (c) show the relation between the number of pulses per burst and the widths of the pulses. These show that pulses tend to be narrower in bursts with more pulses. This may be an intrinsic property of GRBs, or it may be a selection effect arising because narrower pulses have less overlap with adjacent pulses, hence they are easier to resolve, so more pulses tend to be identified in bursts with narrower pulses. This may also be a side effect of correlations between other burst and pulse characteristics with the number of pulses per burst and the pulse widths. Table 4 shows strong negative correlations between the numbers of pulses per fit and the pulse widths. The fits to simulations shown in Figure 19 and Table 16, columns (c) do not have the same tendency. This suggests that the negative correlation between the number of pulses in each fit and the pulse widths seen in the fits to actual bursts do not result from selection effects in the pulse-fitting procedure, but are intrinsic to the burst production mechanism, or may arise from other effects.

3.4.3. Time Delays Between Energy Channels

Table 7, columns (a) show the differences, or time delays, between the peak times $t_{\max}$ of all pulses matched between adjacent energy channels. It shows a significant tendency for individual pulses to peak earlier at higher energies. This has been previously observed, and described as a hard-to-soft spectral evolution of the individual pulses (Norris et al. 1986, 1996). The time delays found here are greater than those found by Norris et al. (1996), who found an average pulse peak time delay between adjacent energy channels of ~ 20 ms. Comparing the peak times of the highest amplitude pulses in each fit between adjacent energy channels also shows a significant tendency for bursts to peak earlier at higher energies. (See Table 7, columns (b).) The time delays between energy channels observed here and elsewhere are likely to result from intrinsic properties of the burst sources.

3.5. Pulse Shapes: Asymmetries and the Peakedness ν

Although the pulse model uses separate rise and decay times as its basic parameters, it is often more natural to consider the widths and asymmetries of pulses, which give equivalent information to the rise and decay times. The ratios of pulse rise times to decay times σ_r/σ_d are a convenient way to measure the asymmetry of pulses, and depends only on the shapes of pulses. The asymmetry

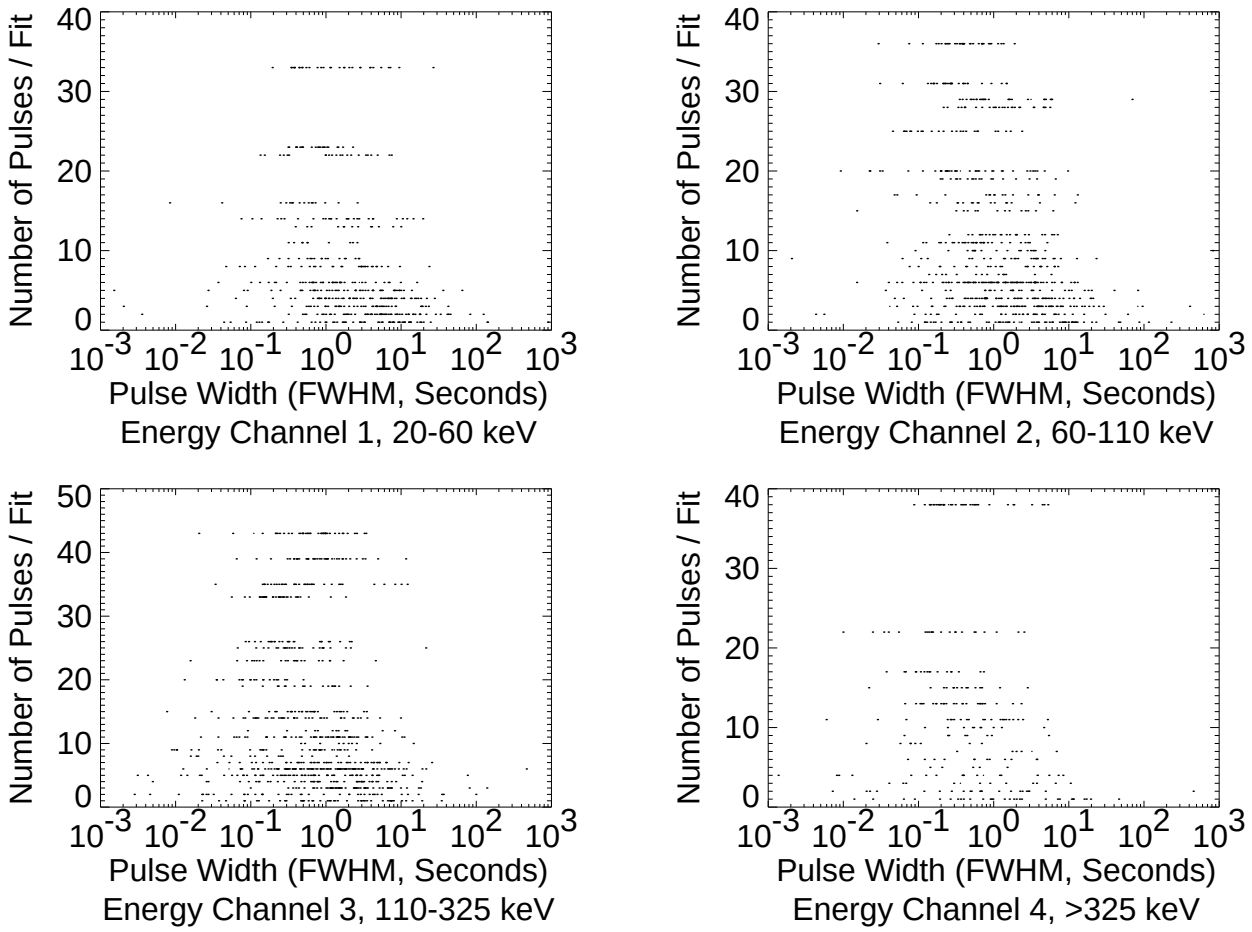

Fig. 8.— Number of pulses per burst versus widths of all pulses from all bursts, by energy channel. Compare with Figure 19 for simulated data. Note that there exists a negative correlation between the two quantities.

Table 7. Characteristics of Distribution of Time Delays Between Adjacent Energy Channels.

	(a) All Matched Pulses			(b) Highest Amplitude Pulse		
Energy Channels	Med. Lag (Sec.)	% > 0	Binom. Prob.	Med. Lag (Sec.)	% > 0	Binom. Prob.
1 - 2	0.11	290/446 = 65%	2.2×10^{-10}	0.08	95/141 = 67%	3.7×10^{-5}
2 - 3	0.27	459/625 = 73%	$< 10^{-16}$	0.05	97/151 = 64%	0.00047
3 - 4	0.01	140/258 = 54%	0.17	0.14	47/67 = 70%	0.00097

ratios cover a very wide range of values, but there is a clear tendency for pulses to have slightly shorter rise times than decay times. (See Figure 9.)

Table 8 shows that the hypothesis that pulses are symmetric is strongly excluded in energy channels 2 and 3. The binomial probability isn't computed for all pulses in all energy channels combined, because pulses cannot be considered to be independent between energy channels. We also see that the degree of the asymmetry isn't significantly different for the different energy channels. Norris et al. (1996) found far greater asymmetry, with average values of σ_d/σ_r (the inverse of the ratio used here) ranging from 2 to 3 for their selected sample of bursts, and with about 90% of pulses having shorter rise times than decay times.

The relation of the peakedness parameter ν to physical characteristics of gamma-ray burst sources is far less clear than for other pulse attributes. Nevertheless, it does give information that can be used to compare the shapes of different pulses. The peakedness ν has a median value near 1.2 in all energy channels, so that pulses tend to have shapes between an exponential, for which $\nu = 1$, and a Gaussian, for which $\nu = 2$. (See Figure 10 and columns (b) of Table 5.) Stern et al. (1997) use the functional form of equation 2 to fit averaged time profiles of many bursts rather than individual constituent pulses, and find that $\nu \approx 1/3$ for the *averaged time profiles*.

4. Correlations Between Pulse Characteristics

Correlations between different characteristics of pulses, or the lack thereof, may reveal much about gamma-ray bursts that the distributions of the individual characteristics cannot. Some correlations may arise from intrinsic properties of the burst sources, while others may result from the differing distances to the sources. The first kind of correlation may be present among pulses of individual bursts or among the whole population of bursts, while the second kind will not be present among pulses of individual bursts. In order to distinguish between these two kinds of effects, it is useful to examine correlations of pulse characteristics both between different bursts, and between pulses within individual bursts.

It is simplest to find correlations between characteristics of all pulses, but such correlations would combine both kinds of effects, and the statistics would be weighted in favor of bursts containing more pulses. It is also possible to select a single pulse from each burst, and find correlations between the characteristics of these pulses from burst to burst in order to look for effects arising from the distances to burst sources. However, if the correlations are taken using the single highest amplitude or highest fluence pulse from each burst, then they could still be affected by correlations of pulse characteristics within individual bursts. For example, consider a situation where amplitudes and durations of pulses within individual bursts are correlated, and where pulse amplitudes and durations follow a common distribution for all bursts. In such a case, if we select the single highest amplitude pulse from each burst, we would find a spurious correlation between highest pulse amplitude and duration between different bursts.

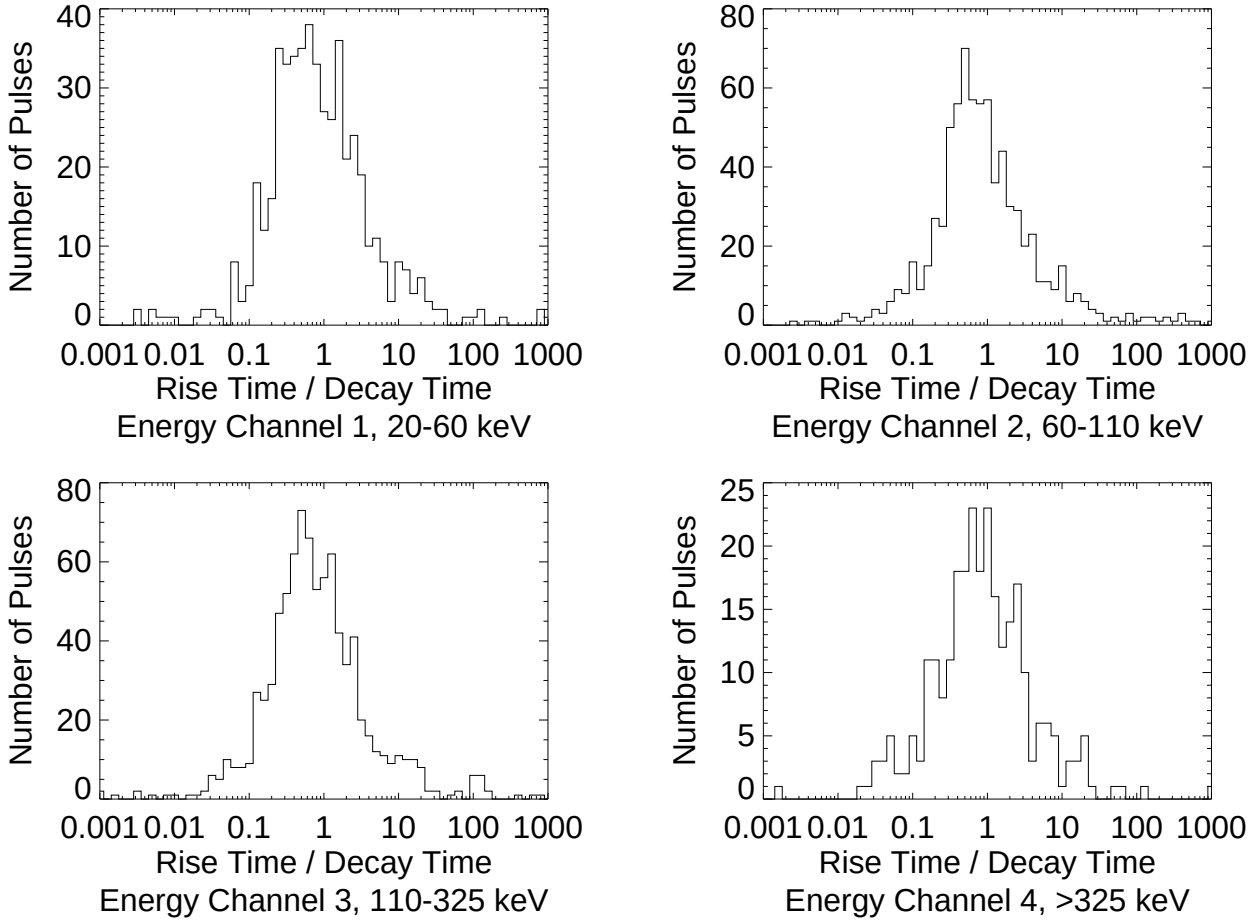

Fig. 9.— Distribution of pulse asymmetry ratios for all pulses from all bursts, by energy channel. See analysis in Table 8.

Table 8. Characteristics of Distribution of Pulse Asymmetries for All Pulses in All Bursts Combined.

Energy Channel	Median σ_r/σ_d	Ratio 84%ile / 16%ile	% $\sigma_r < \sigma_d$	Binom. Prob.
1	0.76	16.8	$297/526 = 56\%$	0.0030
2	0.76	16.1	$457/776 = 59\%$	7.2×10^{-7}
3	0.71	14.0	$528/883 = 60\%$	5.8×10^{-9}
4	0.80	15.9	$158/280 = 56\%$	0.031
All	0.75	15.4	$1440/2465 = 58\%$	···

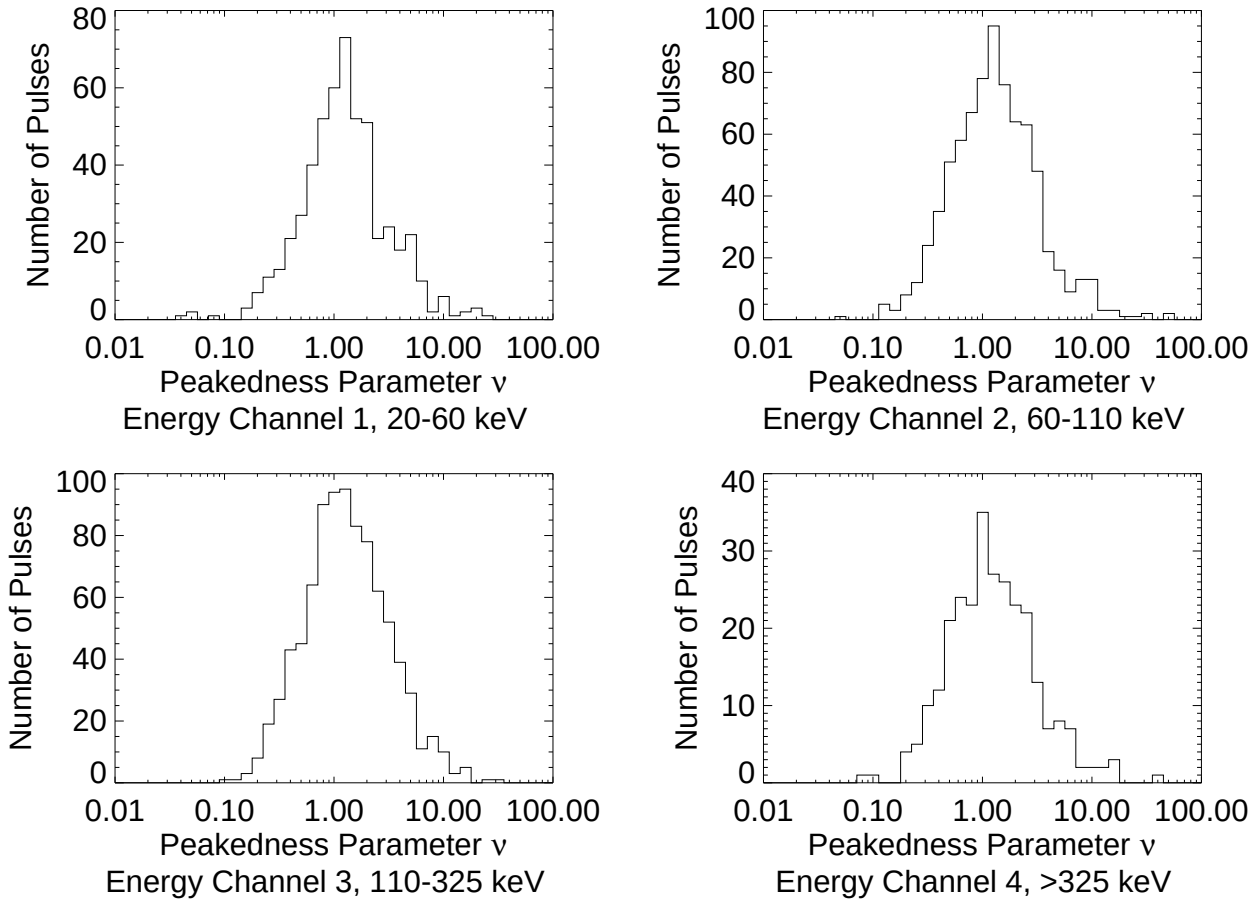

Fig. 10.— Distribution of the peakedness parameter ν for all pulses from all bursts, by energy channel. See analysis in Table 5, columns (b).

Correlation results which compare and contrast the cosmological and intrinsic effects will be discussed in greater detail in the accompanying paper Lee et al. (2000). Here, we describe our method and some other correlation results.

One way to find correlations of pulse characteristics within individual bursts is to calculate a correlation coefficient for each burst and examine the distribution of the degrees of correlation, for example to see if the correlation coefficients were positive for a large majority of bursts. The Spearman rank-order correlation coefficient is used for this purpose here. When using the Spearman rank-order correlation coefficient, the coefficients for the individual bursts are often not statistically significant because the number of pulses in each burst is not large, even though the coefficents for the different bursts may be mostly positive or mostly negative. We can test the hypothesis that there is no correlation because in the absence of any correlation, we would expect an equal number of bursts with positive correlations as with negative correlations, so the probability that the observed numbers of bursts with positive and negative correlations could occur by chance if there was no correlation is given by the binomial distribution. This is the method used here. This method ignores the strengths of the individual correlations, so it is more sensitive to a weak correlation that affects large numbers of bursts than it is to a strong correlation that affects only a small number of bursts.

4.1. Spectral Characteristics

The data that we are using only has very limited spectral information, only four energy channels. We can investigate spectral characteristics by using the *hardness ratios* of individual pulses. The hardness ratio of a pulse between two specified energy channels is the ratio of the fluxes or fluences of the pulse between the two energy channels. Although the actual numerical values of the hardness ratios depend on the somewhat arbitrary boundaries of the energy channels, the values can be compared between different pulses, and between different bursts.

There have been several claims of correlation between peak or average hardness ratios and durations among bursts, with shorter bursts being harder, and there has been some analysis of the cosmological significance of this. Here we investigate similar correlations for bursts, and for pulses in individual bursts.

4.1.1. Pulse Widths

Table 9, columns (a) show the correlations between the pulse amplitude hardness ratios and the pulse widths for the highest amplitude pulse in each burst. The pulse widths used are arithmetic means of the widths in the two adjacent energy channels that the hardness ratios are taken between, *e.g.* hardness ratios between channels 2 and 3 are compared with pulse widths averaged over channels 2 and 3. In all pairs of adjacent energy channels, the highest amplitude pulse has a slight

tendency to be narrower when the burst is harder, as measured using peak flux, but this does not appear to be statistically significant, except possibly between channels 3 and 4. This may be a signature of weak redshift effects; whereby the higher the redshift, the softer the spectrum and the longer the duration.

Table 10, columns (a) shows the correlations between pulse amplitude hardness ratios and pulse widths within bursts. As evident, there is almost equal probability for positive and negative correlations. We conclude, therefore, that there is no significant tendency for longer or shorter duration pulses to have harder or softer spectra, measured using peak flux.

4.1.2. Intervals Between Pulses

Table 9, columns (b) show the correlations between the pulse amplitude hardness ratios and the intervals between the two highest amplitude pulses in each fit. The time intervals used are also averaged over the two adjacent energy channels. In all pairs of adjacent energy channels, the two highest amplitude pulses have a slight tendency to be closer together when the burst is harder (as expected from cosmological redshift effects), as measured using peak flux, but this is not statistically significant, except possibly between channels 1 and 2.

4.1.3. Pulse Amplitudes

Table 9, columns (c) show the correlations between the pulse amplitude hardness ratio and the pulse amplitudes for the highest amplitude pulse in each burst. If the peak luminosity of the highest amplitude pulse is a standard candle or has a narrow distribution, the effects of cosmological redshift would introduce a correlation between hardness ratio and amplitude. In all pairs of adjacent energy channels, the highest amplitude pulse has a slight tendency to be stronger when the burst is

Table 9. Correlations Between Pulse Amplitude Hardness Ratio and (a) Pulse Widths, (b) Intervals Between Two Highest Amplitude Pulses, and (c) Amplitudes for Highest Amplitude Pulse(s) in Each Burst.

Energy	(a) Width		(b) Interval		(c) Amplitude	
Channels	r_s	Prob.	r_s	Prob.	r_s	Prob.
2 / 1	-0.11	0.18	-0.26	0.019	0.01	0.89
3 / 2	-0.21	0.010	-0.06	0.57	0.28	0.00059
4 / 3	-0.41	0.00061	-0.17	0.34	0.31	0.012

harder, as measured using peak flux, but this is not statistically significant (except possibly between channels 2 and 3,) indicating that the distribution of the above-mentioned luminosity is broad.

Table 10, columns (b) shows the correlations between pulse amplitude hardness ratios and pulse amplitudes within bursts. The pulse amplitudes are summed over the two adjacent energy channels that the hardness ratios are taken between. There appears to be no statistically significant tendency for higher amplitude pulses to have harder or softer spectra, although slightly more bursts show a positive correlation (higher amplitude pulses are harder) than a negative correlation (higher amplitude pulses are softer.) This points to a weak or negligible intrinsic correlation between these quantities.

4.1.4. Count Fluence Hardness Ratios

In what follows, we carry out the same tests using the hardness ratio measured by count fluence instead of amplitude, for bursts and pulses within bursts.

Table 11, columns (a) shows the correlations between the total burst count fluence hardness ratios and the pulse widths for the highest amplitude pulses of the bursts. A positive correlation (harder bursts having shorter durations) would be expected if pulse total energy had a narrow intrinsic distribution. There is no consistent or statistically significant tendency for the highest amplitude pulse in each burst to be wider or narrower when the burst is harder or softer, as measured using fluence.

Table 12, columns (a) show the correlations between pulse count fluence hardness ratios and pulse widths within bursts. In channels 1 and 2, more bursts show negative correlations between the two quantities, *i.e.* longer duration pulses tend to have softer spectra, as measured using count fluence, and this effect, which may be statistically significant, indicates the presence of an intrinsic correlation. There are no statistically significant effects between channels 2 and 3 or between

Table 10. Correlations Between Pulse Amplitude Hardness Ratio and (a) Pulse Width and (b) Amplitude Within Bursts.

Energy	(a) Width		(b) Amplitude	
Channels	% Pos. Corr.	Binom. Prob.	% Pos. Corr.	Binom. Prob.
2 / 1	45/83 = 54%	0.44	44.5/83 = 54%	0.51
3 / 2	50/95 = 53%	0.61	49/95 = 52%	0.76
4 / 3	14/33 = 42%	0.38	20.5/33 = 62%	0.16
All	109/211 = 52%	···	114/211 = 54%	···

channels 3 and 4.

Table 11, columns (b) shows the correlations between the total burst count fluence hardness ratios and the intervals between the two highest amplitude pulse in each fit. In all pairs of adjacent energy channels, the two highest amplitude pulses have a slight tendency to be closer together when the burst is harder (as expected from cosmological effects,) but this is not statistically significant.

Table 11, columns (c) shows the correlations between the total burst count fluence hardness ratios and the total burst count fluence in each fit. There is no consistent or statistically significant tendency for harder or softer bursts to contain fewer or more counts.

Table 12, columns (b) shows the correlations between pulse count fluence hardness ratios and pulse count fluences within bursts. The pulse count fluences are summed over the two adjacent energy channels that the hardness ratios are taken between. In channels 1 and 2, more bursts show negative correlations, *i.e.* higher fluence pulses tend to have softer spectra, but again, this intrinsic effect appears weak, and there is no significant effect in the other pairs of energy channels.

In summary, there seems to be little intrinsic correlation between the spectra, as measured by hardness ratio, and other pulse characteristics between bursts and among pulses. There may be weak (statistically not very significant) evidence for trends expected from cosmological redshift effects.

4.2. Time Evolution of Pulse Characteristics Within Bursts

One class of correlations between pulse characteristics within bursts are those between the pulse peak time and other pulse characteristics. These indicate whether certain pulse characteristics tend to evolve in a particular way during the course of a burst. Again, we have used the method described in the previous section, calculating the Spearman rank-order correlation coefficients for the individual bursts, and testing the observed numbers of bursts with positive and

Table 11. Correlations Between Total Burst Count Fluence Hardness Ratio and (a) Pulse Widths, (b) Intervals Between Two Highest Amplitude Pulses, and (c) Total Burst Count Fluences for Highest Amplitude Pulse(s) in Each Burst.

Energy	(a) Width		(b) Interval		(c) Count Fluence	
Channels	r_s	Prob.	r_s	Prob.	r_s	Prob.
2 / 1	0.02	0.84	-0.10	0.36	-0.01	0.88
3 / 2	-0.22	0.0078	-0.07	0.52	0.00	0.98
4 / 3	0.10	0.42	-0.23	0.19	0.21	0.084

negative correlations using the binomial distribution.

4.2.1. Pulse Asymmetry Ratios

Table 13, columns (a) show the number and fraction of bursts (in each channel) where there is a negative correlation between the pulse asymmetry ratio σ_r/σ_d and peak time, *i.e.*, the pulse asymmetry decreases with time. Fits for which the calculated Spearman rank-order correlation coefficient was 0, indicating no correlation, were counted as half for decreasing and half for increasing in order to calculate, using the binomial distribution, the probability of this occurring randomly if pulse amplitudes within bursts are equally likely to increase as to decrease with time. The probability was not calculated for all energy channels combined, because fits to the same burst in different energy channels cannot be considered independent, so the binomial distribution cannot be used.

Pulse asymmetry ratios more often decrease than increase with time during bursts, except in energy channel 4, which has the fewest pulses. This effect appears to be statistically significant in channel 3, and possibly channels 1 and 2. The fits to simulations (See Table 17) show no tendency for pulse asymmetries to increase or decrease within bursts. This indicates that the observed tendency for pulse asymmetry ratios to decrease with time within actual bursts does not arise from selection effects in the pulse-fitting procedure, so that any tendency would be intrinsic to gamma-ray bursts.

4.2.2. Pulse Rise and Decay Times and Pulse Widths

When we examine the evolution of the rise and decay times separately, instead of their ratios, and the evolution of the pulse widths, we find that there is a nearly equal and opposite trend of

Table 12. Correlations Between Pulse Count Fluence Hardness Ratio and (a) Pulse Width and (b) Count Fluence Within Bursts.

Energy	(a) Width		(b) Count Fluence	
Channels	% Pos. Corr.	Binom. Prob.	% Pos. Corr.	Binom. Prob.
2 / 1	52.5/83 = 63%	0.016	51.5/83 = 62%	0.028
3 / 2	47.5/95 = 50%	1.0	47/95 = 49%	0.49
4 / 3	18.5/33 = 56%	0.49	20/33 = 66%	0.61
All	118.5/211 = 56%	···	118.5/211 = 56%	···

decreasing rise times σ_r and increasing decay times σ_d as the burst progresses. This gives rise to the evolution of pulse asymmetry ratios described above, although the statistical significance of the evolution of rise times and decay time are weaker than for the pulse asymmetry ratios. The decrease in rise times is possibly a slightly stronger effect than the increase in decay times. However, the combined effect of these two trends is that there appears to be no statistically significant evolution of pulse widths. (See Table 13, columns (b).) This is in agreement with the results of Ramirez-Ruiz & Fenimore (1999b,a), who found no evidence that pulse widths increase or decrease with time when fitting a power-law time dependence, using a small sample of complex bursts selected from the bright, long bursts fitted by Norris et al. (1996).

4.2.3. Spectra

It has been previously reported that bursts tend to show a hard-to-soft spectral evolution, which we can test by seeing how the hardness ratios of individual pulses vary with time. Table 14, columns (a) show that the pulse amplitude hardness ratios have a slight tendency to decrease with time during bursts between all three pairs of adjacent energy channels. However, with the numbers of available bursts that are composed of multiple pulses in adjacent energy channels, this tendency is statistically insignificant.

4.2.4. Pulse Count Fluences

When we consider the time evolution of the pulse count fluence hardness ratios within bursts, we find no tendency for the hardness ratio of energy channel 2 to channel 1 to increase or decrease, a possibly significant tendency for the hardness ratio of energy channel 3 to 2 to decrease with time, and a statistically insignificant tendency for the hardness ratio of channel 4 to 3 to increase with time. (See Table 14, columns (b).)

4.2.5. Other Pulse Characteristics

We have conducted similar tests for other pulse characteristics and found that none show any tendencies to increase or decrease with time within bursts that are clearly statistically significant (Lee 2000). These pulse characteristics are the pulse amplitude, the peakedness parameter ν, and the pulse count fluence; *e.g.*, we find no tendency for later pulses within a burst to be stronger or weaker, than earlier pulses.

In summary, we find no significant correlations between the peak times of pulses in bursts and any other pulse characteristics except possibly the pulse asymmetry ratio, so that the pulses appear to result from random and independent emission episodes.

Table 13. Correlations Between (a) Pulse Asymmetry Ratio and (b) Width and Pulse Peak Time Within Bursts.

Energy	(a) σ_r/σ_d		(b) Width	
Channel	% Decreasing	Binom. Prob.	% Decreasing	Binom. Prob.
1	61.5/94 = 66%	0.0028	47.5/94 = 51%	0.92
2	66.5/109 = 61%	0.022	60/109 = 55%	0.29
3	81/116 = 70%	1.9×10^{-5}	64/116 = 55%	0.27
4	16/35 = 45%	0.61	23.5/35 = 67%	0.043
All	225/354 = 64%	···	195/354 = 55%	···

Table 14. Correlations Between (a) Pulse Amplitude and (b) Count Fluence Hardness Ratios and Pulse Peak Time Within Bursts.

Energy	(a) Amplitude HR		(b) Count Fluence HR	
Channels	% Decreasing	Binom. Prob.	% Decreasing	Binom. Prob.
2 / 1	46.5/83 = 56%	0.27	42.5/83 = 51%	0.83
3 / 2	54.5/95 = 57%	0.15	61/95 = 64%	0.0056
4 / 3	18.5/33 = 56%	0.48	13/33 = 39%	0.22
All	119.5/211 = 57%	···	116.5/211 = 55%	···

5. Discussion

Decomposing burst time profiles into a superposition of discrete pulses gives a compact representation that appears to contain their important features, so this seems to be a useful approach for analyzing their characteristics. Our pulse decomposition analysis confirms a number of previously reported properties of gamma-ray burst time profiles using a larger sample of bursts with generally finer time resolution than in prior studies. These properties include tendencies for the individual pulses comprising bursts to have shorter rise times than decay times; for the pulses to have shorter durations at higher energies; and for the pulses to peak earlier at higher energies, which is sometimes described as a hard-to-soft spectral evolution of individual pulses.

Pulse rise times tend to decrease during the course of a burst, while pulse decay times tend to increase. When examining pulse widths, or durations, these two effects nearly balance each other; the apparent tendency for pulse widths to decrease during the course of a burst appears to be statistically insignificant. The ratios of pulse rise times to decay times tend to decrease during the course of a burst. The evolution of pulse asymmetry ratios does not arise from selection effects in the pulse-fitting procedure, so it is most likely intrinsic to the bursters.

No other pulse characteristics show any time evolution within bursts, although it is possible that there is non-monotonic evolution; for example, a pulse characteristic may tend to be greater at the beginning and end of a burst and smaller in the middle, and the tests used here wouldn't be sensitive to this. In particular, it doesn't appear that either pulse amplitudes or pulse count fluences have any tendency to increase or decrease during the course of a burst. Also, later pulses in a burst don't tend to be spectrally harder or softer than earlier pulses, although there is spectral softening *within* most pulses. The spectra of pulses within a burst also don't appear to be harder or softer for stronger or weaker pulses, or for longer or shorter duration pulses.

One may therefore conclude that the pulses in a burst arise from random and independent emission episodes such as those expected in the internal episodic shock model rather than the external shock models where the presence of distinguishable pulses must be attributed to inhomogeneities in the interaction of the blast wave shock and the clumpy interstellar medium.

When examining similar correlations between the attributes of some characteristic pulses from burst to burst, we find some weak and tantalizing evidence which may be due to cosmological redshift effects. In the accompanying paper Lee et al. (2000) we describe the correlation studies which can distinguish between trends due to cosmological redshifts and intrinsic trends.

We thank Jeffrey Scargle and Jay Norris for many useful discussions. This work was supported in part by Department of Energy contract DE–AC03–76SF00515.

A. Appendix: Testing for Selection Effects

There are a number of ways in which the pulse-fitting procedure may introduce selection effects into correlations between pulse characteristics. One is that the errors in the different fitted pulse parameters may be correlated. Another is that the pulse-fitting procedure may miss some pulses by not identifying them above the background noise. Still another cause of selection effects is that overlapping pulses may be identified as a single broader pulse.

In order to determine the degree of importance of these selection effects, we have generated a sample of artificial burst time profiles using the pulse model with randomly generated but known pulse parameters, fitted the simulated bursts using the same procedure used for actual burst data, and compared the simulated and fitted pulse characteristics (Lee 2000).

A.1. Numbers of Bursts and Pulses

A total of 286 bursts were generated, with only one energy channel for each burst. For many of these, the limit of 2^{20} counts was reached before the 240 second limit, which almost never occurred in the actual BATSE TTS data. These simulated bursts contained a total of 2671 pulses that had peak times before the limits of 2^{20} counts and 240 seconds, while the fits to the simulated bursts contained a total of only 1029 pulses. Of these, 223 of the simulated bursts and 198 of the fits to the simulations contained more than one pulse. (See Figure 11 and Table 15.) Note that in the fits to actual BATSE data, the largest number of fits containing more than one pulse was 116 for energy channel 3, so that the simulated data set is larger. Figure 12 shows the number of pulses fitted versus the number of pulses originally generated for each simulated bursts. It shows that the greatest differences between the the fitted and the simulated numbers of pulses tend to occur in the most complex bursts. Figure 13 compares the numbers of pulses per fit between the simulations and the fits to simulations. Most (54%) of the fits to simulated bursts contain fewer pulses than the initial simulations, and for nearly all of the remaining simulated bursts, the number of pulses are the same for the initial simulations and the fits to simulations. The fits to simulations have a mean of 15 fewer pulses than the initial simulations, and a median of 1 fewer pulse. The fits to simulations have a geometric mean of 0.63 times as many pulses as the initial simulations, and a mean of 0.80 times as many pulses.

A.2. Brightness Measures of Simulated Pulses

Figure 14 shows the distribution of pulse amplitudes in the original simulations and in the fits to simulations. It shows that the fitting procedure has a strong tendency to miss low amplitude pulses. However, if we compare this with Figure 3, we see that in the fits to actual BATSE bursts, the fitting procedure found pulses with considerably lower amplitudes than it found in the fits to

Table 15. Characteristics of Distribution of Number of Pulses in Simulations.

	Median No. of Pulses	Mean No. of Pulses	Max. No. of Pulses	% Single Pulse
Simulation	3	9.3	126	62/286 = 22%
Fit to Sim.	2	3.6	19	88/286 = 31%

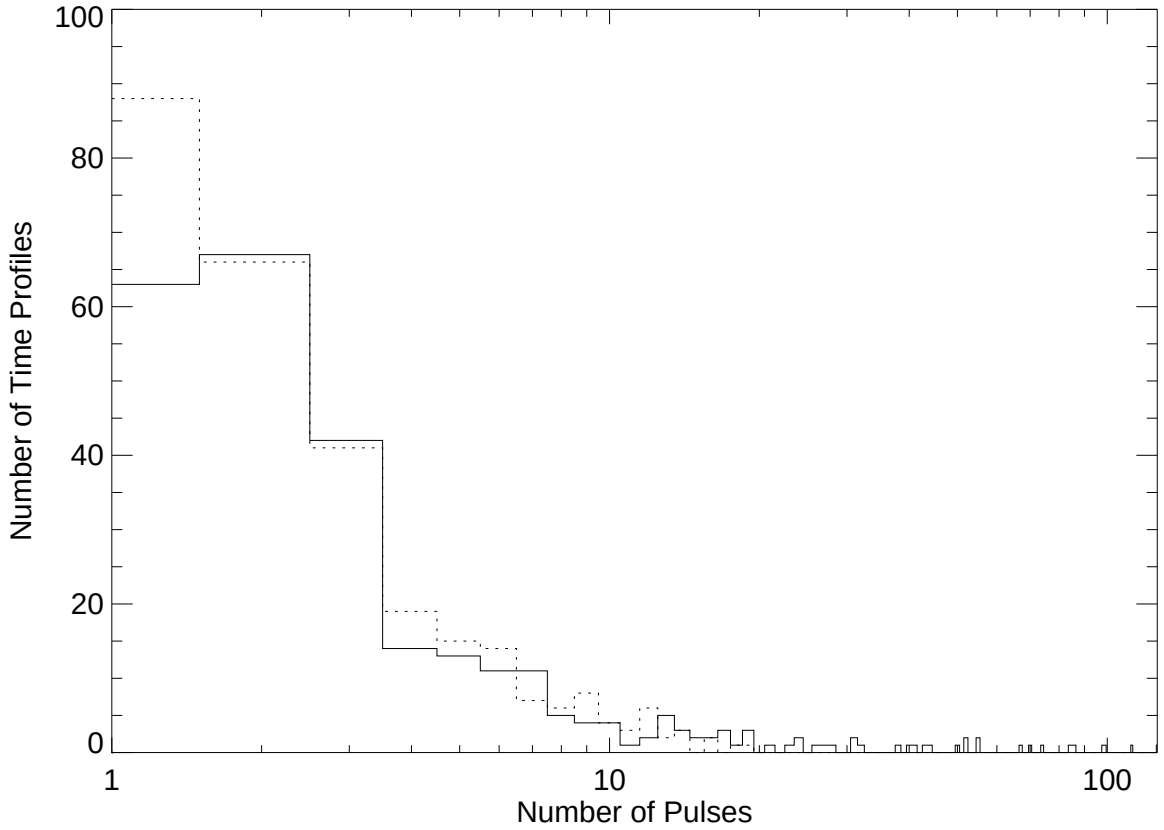

Fig. 11.— Distribution of number of pulses in initial simulations (solid histogram) and in the results of the fits to the simulated data (dashed histogram).

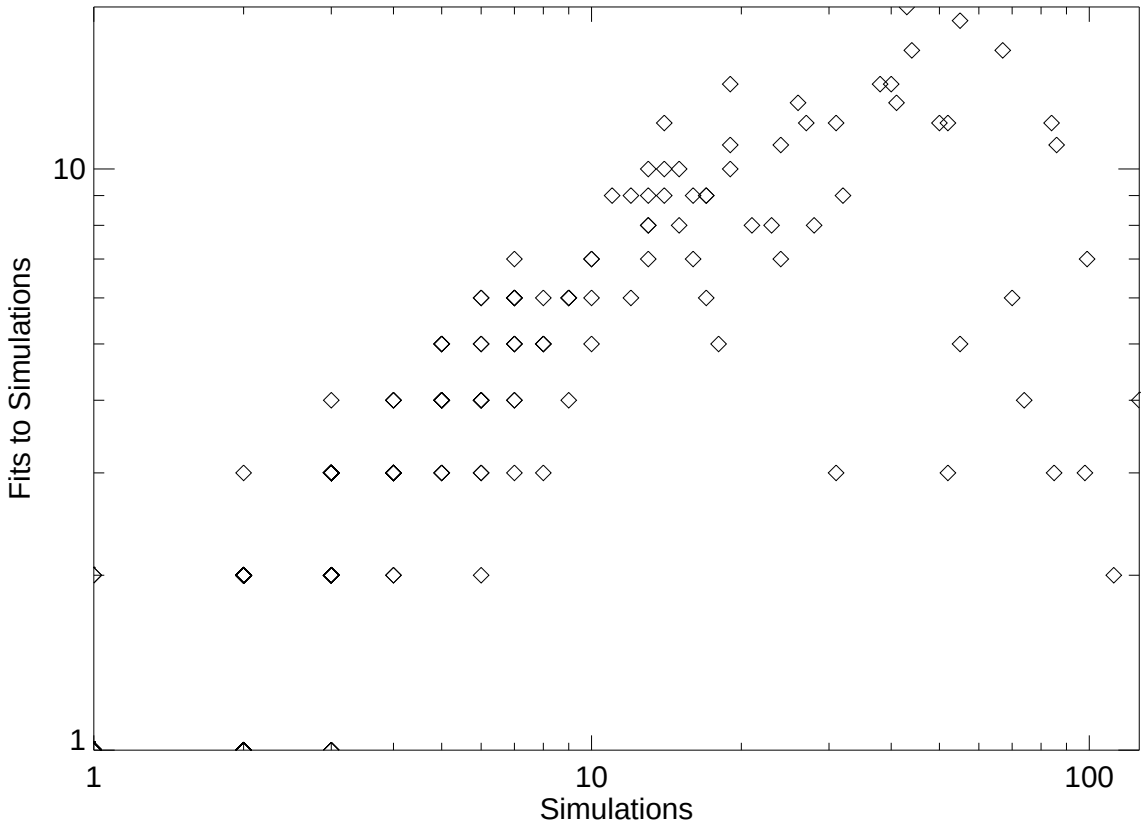

Fig. 12.— Number of pulses obtained from fits to the simulations versus number in the initial simulations. Note that the selection effect of the fitting procedure is more pronounced in bursts with larger numbers of pulses.

simulated bursts.

Figure 15 shows the number of pulses in each burst plotted against the amplitudes of all of the pulses comprising each fit. In the simulations, there are no correlations between pulse amplitudes and the number of pulses in the time profile, because the pulse amplitudes were generated independently of the number of pulses in each burst. In the fits to the simulations, pulse amplitudes tend to be higher in bursts containing more pulses. This must result from the selection effect discussed in Section 3.3; it is easier to identify more pulses when they are stronger. Table 16, columns (a) shows that even though there is no correlation between pulse amplitudes and the number of pulses for the initial simulated data, the fitting procedure introduces a strong positive correlation between these quantities; the tendency to miss low amplitude pulses is greater in more complex bursts.

Figure 16 shows the distribution of pulse count fluences in the original simulations and in the fits to simulations. It shows that the fitting procedure has a strong tendency to miss pulses with low count fluences, similar to what we have seen for low amplitude pulses.

Figure 17 and Table 16, columns (b) compare the number of pulses in each time profile with the count fluences of the individual pulses. They show no tendency for pulses to contain fewer or more counts in bursts with more pulses, in either the initial simulations (by design) or in the fits to simulations. Unlike pulse amplitudes, the tendency to miss low count fluence pulses appears to be independent of burst complexity. This differs from the results seen in the fits to actual bursts, where bursts containing more pulses tended to have pulses with lower count fluences. (See Figure 6 and Table 4, columns (b).) This may explain why the 2^{20} count limit for the TTS data was frequently reached before the 240 second time limit in the simulated bursts, but rarely in the actual bursts; the total count fluence increases linearly with the number of pulses in the simulated bursts, but less rapidly in the actual BATSE bursts.

Table 16. Correlation Between Number of Pulses per Burst and (a) Amplitudes, (b) Count Fluences, and (c) Widths of All Pulses in Simulated Bursts.

	(a) Amplitude		(b) Count Fluence		(c) Width	
	r_s	Prob.	r_s	Prob.	r_s	Prob.
Simulation	-0.04	0.042	-0.02	0.31	0.01	0.76
Fit to Sims.	0.22	7.1×10^{-13}	0.11	0.00068	-0.03	0.36

A.3. Pulse Widths

Figure 18 shows the distribution of pulse widths in the original simulations and in the fits to simulations. The pulses in the fits to simulations tend to be slightly longer in duration than in the original simulations, but applying the Kolmogorov-Smirnov test to the two distributions show that they are not significantly different; the probability that they are the same distribution is 0.39. This agrees with what we have seen in Figures 14 and 16, that the selection effects of the fitting procedure for pulse amplitudes and for pulse count fluences are similar.

Figure 19 and Table 16, columns (c) compare the number of pulses in each time profile with the widths of the individual pulses. They show no tendency for pulses to be wider or narrower in bursts with more pulses, in either the simulations or the fits to the simulations.

A.4. Time Evolution of Pulse Characteristics Within Bursts

In the fits to actual BATSE data, it was found that pulse asymmetry ratios tended to decrease over the course of a burst. (See Table 13.) Table 17 shows the correlations between pulse asymmetry ratio and peak times within bursts for the simulations and the fits to simulations. It shows no tendency for positive or negative correlations in either the simulations or the fits to simulations.

REFERENCES

Donoho, D. L. 1992, De-Noising via Soft Thresholding, Department of Statistics Technical Report 409, Stanford University, Stanford, CA

Fenimore, E. & Bloom, J. 1995, ApJ, 453, 25

Kouveliotou, C., Briggs, M. F., & Fishman, G. J., eds. 1996, Gamma-Ray Bursts: 3rd Huntsville Symposium, AIP Conf. Proc. No. 384 (Woodbury, NY: AIP)

Kouveliotou, C. et al. 1993, ApJ, 413, L101

Table 17. Correlations Between Pulse Asymmetry Ratio and Pulse Peak Time Within Simulated Bursts.

	% Decreasing	Binom. Prob.
Simulation	92.5/223 = 41%	0.016
Fit to Sim.	103/198 = 52%	0.57

Lee, A. 2000, PhD thesis, Stanford University, Stanford, CA, (SLAC–R–553)

Lee, A., Bloom, E. D., & Petrosian, V. 2000, ApJ, submitted, (SLAC–PUB–8365)

Lee, A., Bloom, E. D., & Scargle, J. D. 1996, in Gamma-Ray Bursts: 3rd Huntsville Symposium, ed. C. Kouveliotou, M. F. Briggs, & G. J. Fishman, AIP Conf. Proc. No. 384 (Woodbury, NY: AIP), 47–51

Lee, A., Bloom, E. D., & Scargle, J. D. 1998, in Gamma-Ray Bursts: 4th Huntsville Symposium, ed. C. A. Meegan, R. D. Preece, & T. M. Koshut, AIP Conf. Proc. No. 428 (Woodbury, NY: AIP), 261–265

Link, B., Epstein, R. I., & Priedhorsky, W. C. 1993, ApJ, 408, L81

Meegan, C. A. 1991, BATSE Flight Software User's Manual, NASA/MSFC, Huntsville, AL

Meegan, C. A. et al. 1996a, in Gamma-Ray Bursts: 3rd Huntsville Symposium, ed. C. Kouveliotou, M. F. Briggs, & G. J. Fishman, AIP Conf. Proc. No. 384 (Woodbury, NY: AIP), 291–300

Meegan, C. A. et al. 1996b, ApJS, 106, 65

Norris, J. P. et al. 1986, ApJ, 301, 213

—. 1996, ApJ, 459, 393

Ramirez-Ruiz, E. & Fenimore, E. 1999a, ApJ, submitted, (astro-ph/9910273)

—. 1999b, A&AS, 138, 521

Stern, B., Poutanen, J., & Svensson, R. 1997, ApJ, 489, L41

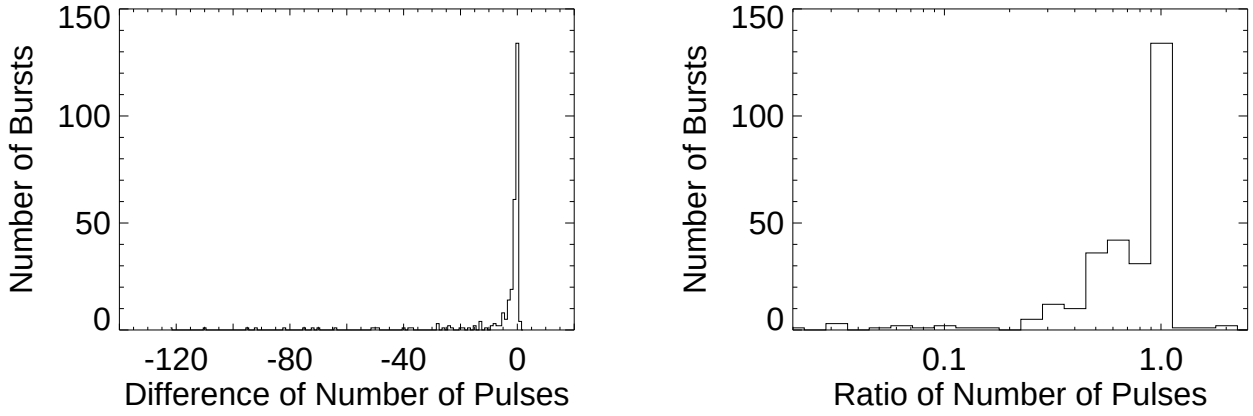

Fig. 13.— (Left) Distribution of differences between numbers of pulses from initial simulated bursts to fits to simulated bursts. A small number of bursts have many fewer pulses in the fits to simulations than in the initial simulations. (Right) Distribution of ratios of numbers of pulses from initial simulated bursts to fits to simulated bursts.

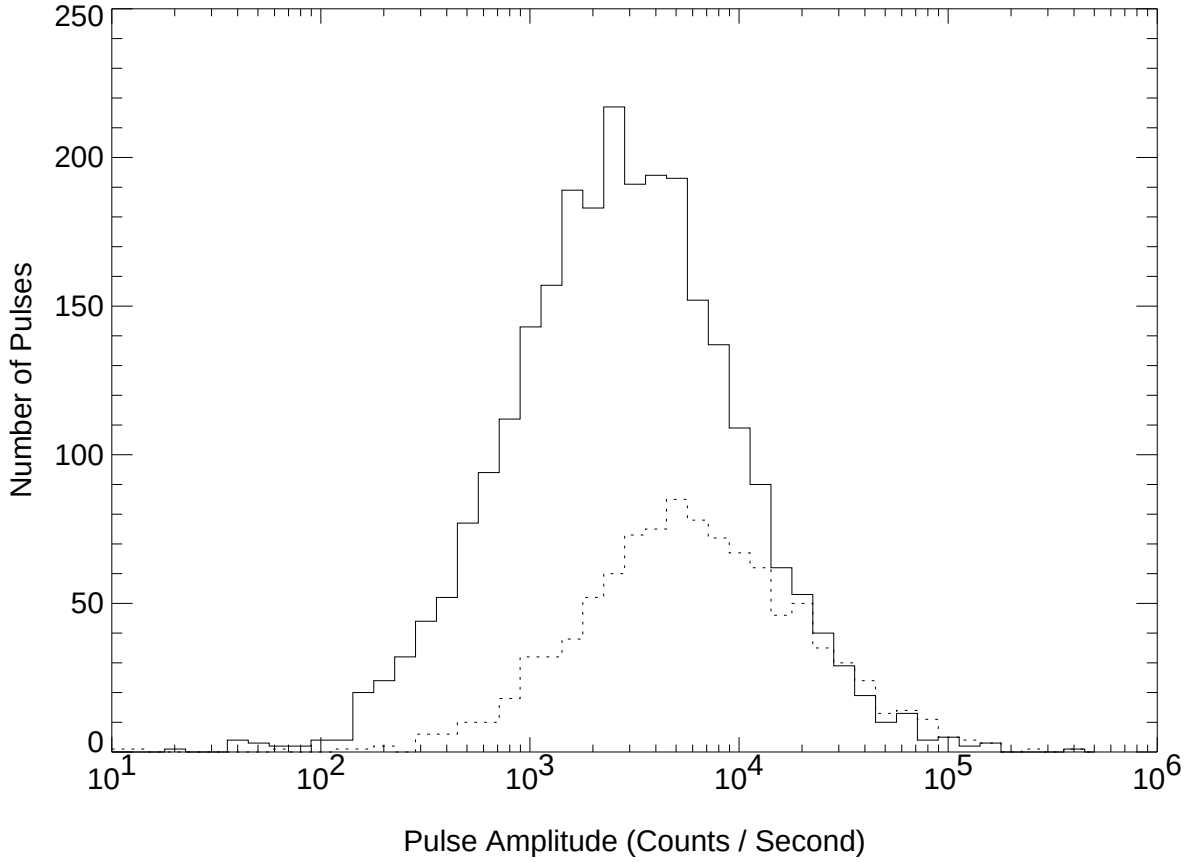

Fig. 14.— Distribution of pulse amplitudes for all pulses from all bursts in initial simulations (solid histogram) and in the results of the fits to the simulated data (dashed histogram).

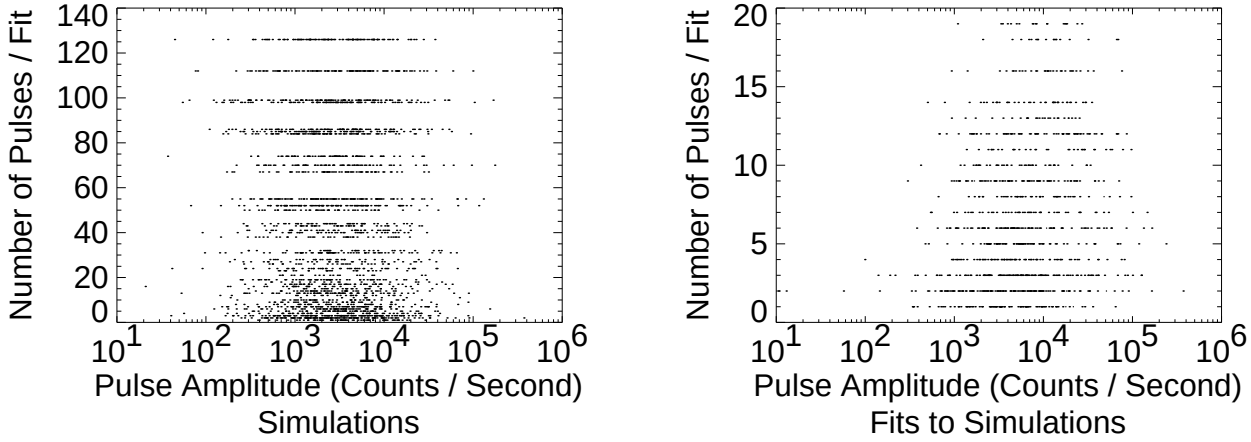

Fig. 15.— Number of pulses per fit versus pulse amplitudes of all pulses.

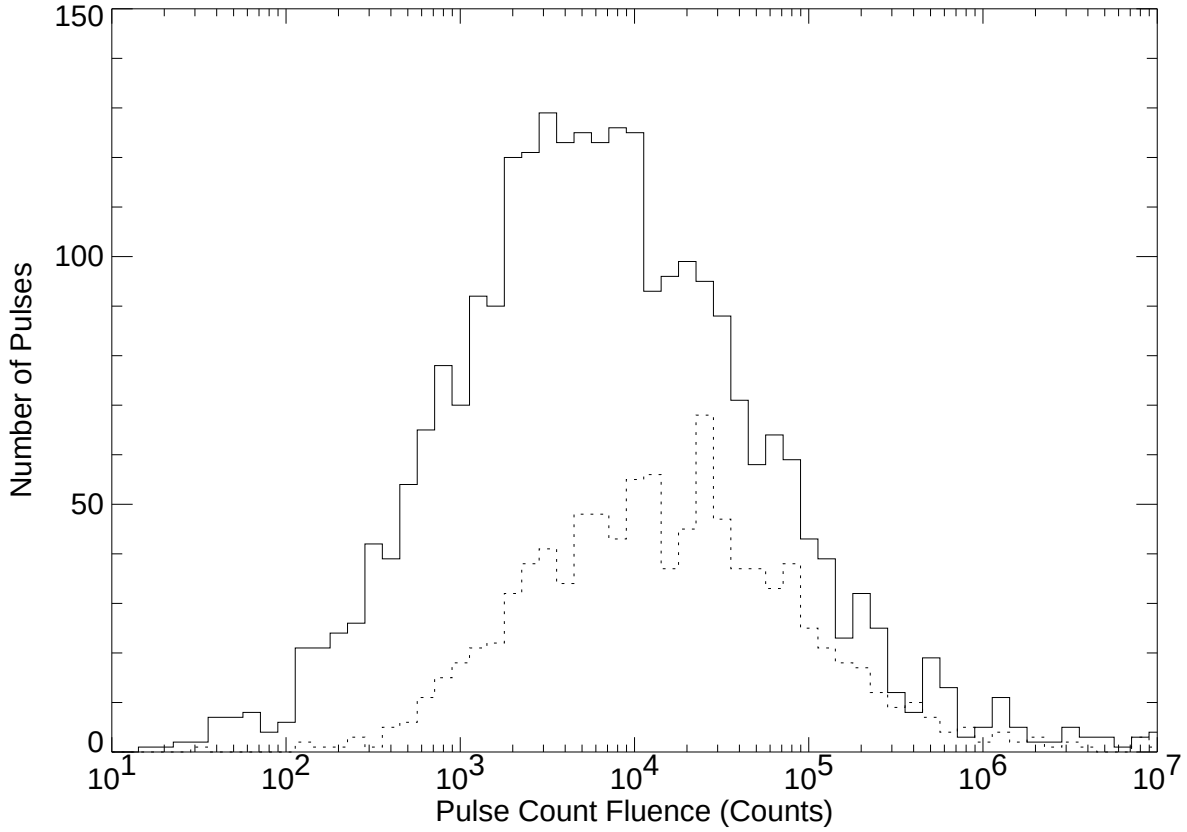

Fig. 16.— Distribution of pulse count fluences for all pulses from all bursts in initial simulations (solid histogram) and in the results of the fits to the simulated data (dashed histogram).

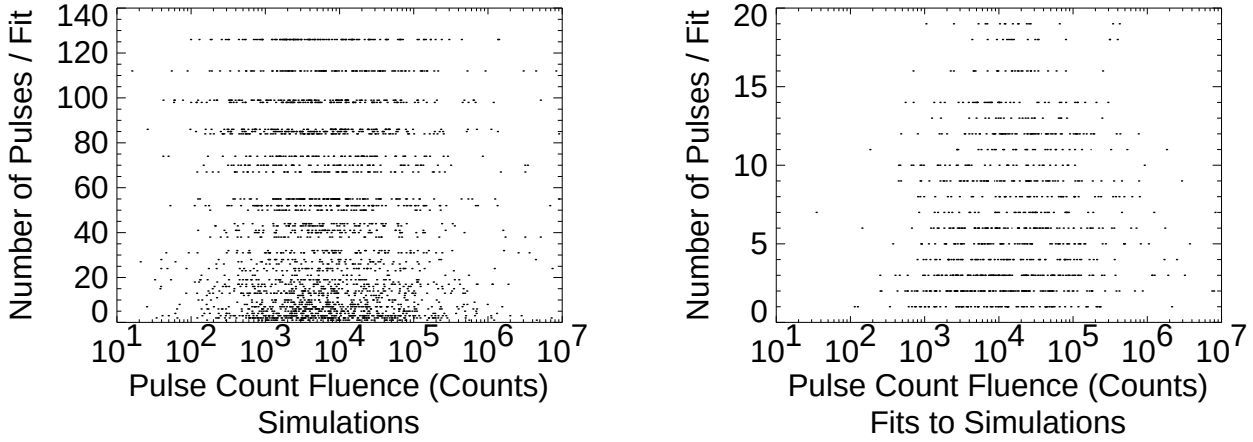

Fig. 17.— Number of pulses per burst versus count fluences of all pulses.

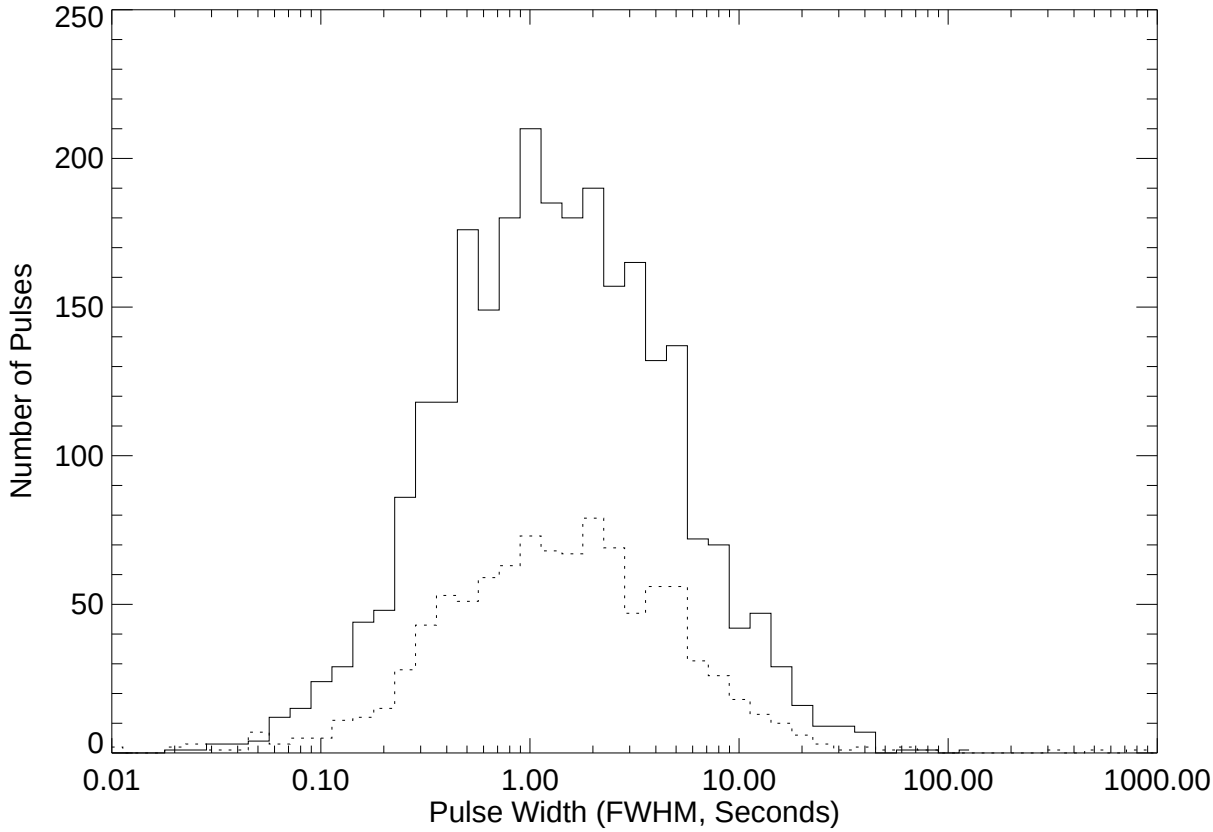

Fig. 18.— Distribution of pulse widths for all pulses from all bursts in initial simulations (solid histogram) and in the results of the fits to the simulated data (dashed histogram).

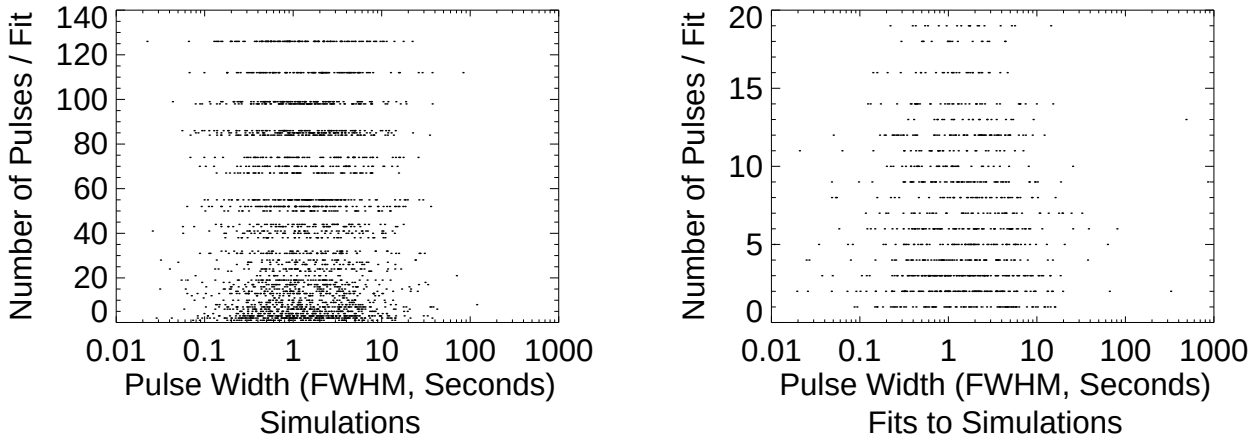

Fig. 19.— Number of pulses per burst versus widths of all pulses.